Neuropharmacology 205 (2022) 108914

Contents lists available at ScienceDirect

Neuropharmacology

journal homepage: www.elsevier.com/locate/neuropharm

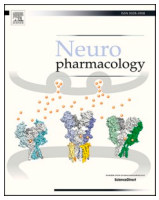

Preclinical investigation of β-caryophyllene as a therapeutic agent in an experimental murine model of Dravet syndrome

Cristina Alonso [a,b,c], Valentina Satta [a,b,c], Paula Díez-Gutiérrez [a], Javier Fernández-Ruiz [a,b,c,1,*], Onintza Sagredo [a,b,c,**,1]

[a] Instituto Universitario de Investigación en Neuroquímica, Departamento de Bioquímica y Biología Molecular, Facultad de Medicina, Universidad Complutense, Madrid, Spain
[b] Centro de Investigación Biomédica en Red de Enfermedades Neurodegenerativas (CIBERNED), Madrid, Spain
[c] Instituto Ramón y Cajal de Investigación Sanitaria (IRYCIS), Madrid, Spain

ARTICLE INFO

Keywords:
Dravet syndrome
Infantile epileptic refractory syndromes
Syn-Cre/Scn1a$^{WT/A1783V}$ mice
Cannabinoids
β-caryophyllene
Seizuring activity
Behavioural comorbidities
Glial reactivity

ABSTRACT

Dravet Syndrome (DS) is caused by mutations in the *Scn1a* gene encoding the α1 subunit of the sodium channel Nav1.1, which results in febrile seizures that progress to severe tonic-clonic seizures and associated comorbidities. Treatment with cannabidiol has been approved for the management of seizures in DS patients, but it appears to be also active against associated comorbidities. In this new study, we have investigated β-caryophyllene (BCP), a cannabinoid with terpene structure that appears to also have a broad-spectrum profile, as a useful therapy against both seizuring activity and progression of associated comorbidities. This has been studied in heterozygous conditional knock-in mice carrying a missense mutation (A1783V) in *Scn1a* gene expressed exclusively in neurons of the Central Nervous System (Syn-Cre/Scn1a$^{WT/A1783V}$), using two experimental approaches. In the first approach, an acute treatment with BCP was effective against seizuring activity induced by pentylenetetrazole (PTZ) in wildtype (Scn1a$^{WT/WT}$) and also in Syn-Cre/Scn1a$^{WT/A1783V}$ mice, with these last animals having a greater susceptibility to PTZ. Such benefits were paralleled by a BCP-induced reduction in PTZ-induced reactive astrogliosis (labelled with GFAP) and microgliosis (labelled with Iba-1) in the prefrontal cortex and the hippocampal dentate gyrus, which were visible in both wildtype (Scn1a$^{WT/WT}$) and Syn-Cre/Scn1a$^{WT/A1783V}$ mice. In the second approach, both genotypes were treated repeatedly with BCP to investigate its effects on several DS comorbidities. Thus, BCP corrected important behavioural abnormalities of Syn-Cre/Scn1a$^{WT/A1783V}$ mice (e.g. delayed appearance of hindlimb grasp reflex, induction of clasping response, motor hyperactivity, altered social interaction and memory impairment), attenuated weight loss, and slightly delayed premature mortality. Again, these benefits were paralleled by a BCP-induced reduction in reactive astrogliosis and microgliosis in the prefrontal cortex and the hippocampal dentate gyrus typical of Syn-Cre/Scn1a$^{WT/A1783V}$ mice. In conclusion, BCP was active in Syn-Cre/Scn1a$^{WT/A1783V}$ mice against seizuring activity (acute treatment) and against several comorbidities (repeated treatment), in both cases in association with its capability to reduce glial reactivity in areas related to these behavioural abnormalities. This situates BCP in a promising position for further preclinical evaluation towards a close translation to DS patients.

1. Introduction

Dravet syndrome (DS) (ORPHA: 33069; OMIM: 607208), also known as severe myoclonic epilepsy of infancy (SMEI), is a rare pediatric encephalopathy that typically begins in the first year of life in a child with prior diagnosis apparently normal, giving rise to a devastating long-term outcome (Gataullina and Dulac, 2017). It accounts for 1.4% of children with epilepsy, with an average incidence estimated in 1:20,000 births (Wu et al., 2015). Nearly 80% of patients carry de novo mutations in the gene *Scn1a*, which encodes the α1 subunit of the voltage-gated sodium channel ($Na_V1.1$) (Marini et al., 2011). DS patients usually present heterozygous loss-of-function mutations triggering haploinsufficiency,

* Corresponding author. Department of Biochemistry and Molecular Biology, Faculty of Medicine, Complutense University, 28040, Madrid, Spain.
** Corresponding author. Department of Biochemistry and Molecular Biology, Faculty of Medicine, Complutense University, 28040, Madrid, Spain.
E-mail addresses: jjfr@med.ucm.es (J. Fernández-Ruiz), onintza@med.ucm.es (O. Sagredo).
[1] Both authors shared the last position within authorship and act as corresponding authors

https://doi.org/10.1016/j.neuropharm.2021.108914
Received 19 July 2021; Received in revised form 29 November 2021; Accepted 1 December 2021
Available online 4 December 2021

which severely impairs sodium currents and action potential firing in GABAergic inhibitory interneurons. This leads to a decreased GABAergic neurotransmission and, subsequently, a marked hyperexcitability in neuronal circuits which results in the complex DS phenotype (Bender et al., 2012). A large body of evidence has demonstrated that DS is clinically characterized by multiple treatment-resistant seizure types and frequent status epilepticus that contribute, although it is not the unique cause in the development of long-term comorbidities (including cognitive impairment, hyperactivity and autistic traits), and a higher incidence of sudden premature death (Dravet, 2011).

Defining appropriate therapeutic strategies is pivotal, since it is a chronic, progressive and devastating disorder. Just after diagnosis, first-line therapies often include valproic acid and clobazam. If needed, second-line therapies such as topiramate and stiripentol can be added as adjuvants to improve the response (Wirrell et al., 2017). However, therapeutic management usually remains inadequate and can be associated with undesirable side effects, thus making essential the development of new and effective therapies against epileptic episodes. In addition, an effective therapy against long-term comorbidities, beyond the control of seizuring activity, is still lacking. In the search of new treatments, recent arrivals are fenfluramine (approved in 2020 by the US Food and Drug Administration (FDA); Sullivan and Simmons, 2021), and, in particular, cannabidiol (CBD), a specific constituent of *Cannabis Sativa*, which may target directly or indirectly the so-called endocannabinoid system and/or external pharmacological targets (Rosenberg et al., 2015).

The interest of CBD as an antiseizuring treatment for DS children was initiated in 2013, when a group of parents of children affected by DS and other treatment-resistant pediatric epilepsies reported positive experiences after treating their children with artisanal CBD-enriched oral products (Porter and Jacobson, 2013). In light of these promising effects, an oral CBD formulation was marked as Epidiolex® by the British company GW Pharmaceuticals and obtained orphan designation by regulatory agencies for developing sponsored clinical trials (Devinsky et al., 2016, 2017). Its efficacy and good tolerability led to the recent approval of Epidiolex® by the two main regulatory agencies, i.e., the US FDA and the European Medicines Agency (EMA), as an anticonvulsant agent for the treatment of patients with DS, Lennox-Gastaut and similar refractory pediatric epileptic syndromes (Franco et al., 2021). However, the underlying mechanisms mediating CBD therapeutic effects (antiseizuring activity) in these children still remain unknown, with some proposals still pending to be confirmed: e.g. targeting TRPV1 receptors (Gray et al., 2020). By contrast, it is generally accepted that certain benefits could arise from its well-demonstrated anti-inflammatory, antioxidant and cytoprotective properties (Fernández-Ruiz et al., 2013), which may be particularly useful for long-term comorbidities found in DS patients (Villas et al., 2017; Lagae et al., 2018). In fact, in the first attempt trying to elucidate this mechanism(s), CBD proved beneficial effects (antiseizuring but also attenuating associated comorbidities) in *Scn1a*$^{+/-}$ mice, which appeared to be mediated, at least in part, by GPR55, an orphan GPCR that has been related to the endocannabinoid system (Kaplan et al., 2017). Follow-up studies confirmed this potential of CBD against premature mortality and behavioural comorbidities in preclinical models (Patra et al., 2020).

In recent years, other cannabis constituents have also shown to exert antiseizuring properties in experimental epilepsy models including DS (Perucca, 2017; Anderson et al., 2019). An example is β-caryophyllene (BCP), a sesquiterpene abundantly found in the essential oils (about 35%) of *Cannabis Sativa* (da Fonsèca et al., 2019). BCP was first described as a full and selective agonist of cannabinoid type-2 (CB_2) receptors (Gertsch et al., 2008), but further studies have demonstrated that it is also able to activate peroxisome proliferator-activated receptor (PPAR)-α/γ and μ-opioid receptors, as well as to inhibit homomeric nicotinic acetylcholine receptors (α7-nAChRs) and the toll-like receptor complex (CD14/TLR4/MD2) (Sharma et al., 2016). This polypharmacological nature allows BCP to exert multiple pharmacological activities, showing antioxidant, anti-inflammatory, anticonvulsant, analgesic and neuroprotective properties, among others (Sharma et al., 2016). Similarly to CBD, BCP is devoid of the psychoactive side effects associated with cannabinoid type-1 (CB_1) receptor activation, thus making BCP a novel candidate for a wide variety of therapeutic applications (Sharma et al., 2016; Gonçalves et al., 2020). This also includes seizures, as BCP has been shown to display antiepileptic effects in different animal models of epilepsy, as well as to attenuate inflammatory processes which are typically linked to hyperexcitability (Liu et al., 2015; de Oliveira et al., 2016; Tchekalarova et al., 2018).

With these last ideas in mind, the present study was designed to evaluate the possible beneficial effects of BCP in DS. Given the complex DS phenotype, we evaluated BCP effects not only against seizuring activity, but also, and in particular, against associated comorbidities. To this end, we used a heterozygous conditional knock-in mouse model carrying a missense mutation (A1783V) in the *Scn1a* gene, which has been previously characterized by our group (Satta et al., 2021). We used two different experimental paradigms in these mice: (i) an acute approach aimed at investigating the anticonvulsant effect of BCP against seizuring activity induced by the proconvulsive agent pentylenetetrazole (PTZ); and (ii) a longer treatment aimed at evaluating BCP benefits on the disease progression and associated comorbidities. In both cases, the behavioural analyses were accompanied by an evaluation, using immunostaining, of the potential of BCP against inflammation induced by PTZ in the acute paradigm or generated by the progression of the pathological phenotype in the conditional knock-in mouse model of DS used in this study.

2. Materials and methods

2.1. Animals and genotyping

We used conditional knock-in mutant mice (knock-in mutation A1783V in Nav1.1 protein) generated by Cre-*loxP* technology, in which the *Scn1a* gene is primarily mutated in neuronal cells. With this purpose, B6(Cg)-Scn1atm1.1Dsf/J mice (heterozygous for the transgene, JAX stock #026133) were crossed with Cre-recombinase linked to synapsin-1 promoter mice (CreB6.Cg-Tg(Syn1-cre)671Jxm/J; JAX stock #003966), both in C57BL6/J background and acquired from The Jackson Laboratory (Bar Harbor, ME, USA), breedings which gave rise to offspring in one of the four following experimental groups: the Syn-Cre/Scn1a$^{WT/A1783V}$ mice, which bear the A1783V mutation in Nav1.1 protein exclusively in Central Nervous System (CNS) neurons, showing the pathological phenotype, and their three different control mice, Scn1a$^{WT/WT}$ (wild-type not expressing Cre), Syn-Cre/Scn1a$^{WT/WT}$ (wild-type expressing Cre) and Scn1a$^{WT/A1783V}$ (A1783V mutant not expressing Cre). Since our previous study (Satta et al., 2021) aimed at characterizing this murine model indicated that these three different control mice show, in general, a normal phenotype, for this new study, we have worked with Scn1a$^{WT/WT}$ mice as the unique control group. Approximately 15 litters were needed to generate the number of animals required for the experiments projected in these two genotypes, and, in both cases, all animals born in each litter were proportionally distributed for the two genotypes and the 2–3 treatment groups. In addition, given that the incidence and severity of this disease is similar in children irrespective of the gender (Skluzacek et al., 2011), and that we found this also happened in this experimental murine model in our previous study (Satta et al., 2021), our experimental groups for this new study were formed with equivalent proportions of male and female mice in all cases. Genotypes were verified by polymerase chain reaction (PCR) using genomic DNA from mouse tail biopsies. Genomic DNA was extracted and amplified using REDExtract-N-Amp Tissue PCR kit (Sigma-Aldrich, Madrid, Spain), following manufacturer's instructions and as published elsewhere (Satta et al., 2021).

As aforementioned, mice from both genotypes were used for two different experiments: (i) an acute approach aimed at investigating the

anticonvulsant effect of BCP against seizuring activity induced by the proconvulsive agent PTZ in both Scn1a$^{WT/WT}$ and Syn-Cre/Scn1a$^{WT/A1783V}$ mice; and (ii) a longer treatment aimed at evaluating BCP benefits on the disease progression and associated comorbidities in Syn-Cre/Scn1a$^{WT/A1783V}$ mice compared to Scn1a$^{WT/WT}$ animals. During both experiments, mice were housed in a climate-controlled room (21 ± 2 °C and 60% humidity) under a controlled photoperiod of 12 h light/12 h dark (08:00–20:00 light). All animals had *ad libitum* access to standard chow and water. All experiments were conducted according to national and European guidelines (RD 53/2013 and directive 2010/63/EU, respectively), followed the principles of the ARRIVE and 3R guidelines, and were approved by the Animal Welfare Committee of the Complutense University and the "Comunidad de Madrid" (ref. PROEX 033/17). All possible efforts were made to minimize animal pain and discomfort, as well as reduce the number of experimental subjects.

2.2. Experiment #1 (acute): pharmacological treatment, behavioural recording and sampling

Seizuring activity was induced by administration of the proconvulsant PTZ (Sigma-Aldrich, Madrid, Spain), following a previous method (Alachkar et al., 2020), to both Scn1a$^{WT/WT}$ and Syn-Cre/Scn1a$^{WT/A1783V}$ mice at PND24. To investigate the BCP effect on PTZ-induced seizuring activity, mice were individually placed in glass boxes and injected with a single dose of BCP (100 mg/kg, i.p.) or its vehicle (0.9% NaCl containing 2% Tween 80). 30 min thereafter, mice were injected with PTZ (50 mg/kg, i.p.) and were then observed for a 30-min period. Before administration, PTZ was freshly dissolved in sterile saline (0.9% NaCl) to prepare a solution with a concentration of 10 mg/ml. During this 30-min period, several behavioural parameters were recorded: (i) latency to myoclonic jerks, (ii) latency to generalized seizures, (iii) the difference between both latencies (calculated as latency to generalized seizures minus latency to myoclonic jerks for each animal), and (iv) total duration of generalized seizures, following the procedure described by Alachkar et al. (2020). PTZ dose and experimental schedule were selected based on pilot experiments. Boxes were cleaned with 70% alcohol prior to the next session to remove residual odors and any olfactory interference. 24 h after PTZ injection (at PND25), mice were euthanized by rapid decapitation and brains were rapidly removed and fixed for one day at 4 °C in fresh 4% paraformaldehyde prepared in 0.1 M phosphate buffered-saline (PBS), pH 7.4, then cryoprotected by immersion in a 30% sucrose solution for a further day, and finally stored at −80 °C for immunofluorescence analysis.

2.3. Experiment #2 (repeated): pharmacological treatment, behavioural recording and sampling

To evaluate the potential of BCP against the disease progression and associated comorbidities in Syn1-Cre/Scn1a$^{WT/A1783V}$ mice, animals with this genotype and their controls (Scn1a$^{WT/WT}$ mice) were treated with BCP at a dose of 10 mg/kg administered i.p. or its vehicle (0.9% NaCl containing 2% Tween 80). The treatment started at PND10 and injections were given every 48 h (even days) up to PND24. The option of a treatment in alternate days was selected given the extreme vulnerability of Syn1-Cre/Scn1a$^{WT/A1783V}$ mice due to their immaturity (this also applied to Scn1a$^{WT/WT}$ mice) and evident disabilities, which recommended to avoid the stress of daily injections of either BCP or vehicle). During this treatment period, body weight was measured daily whereas the maturation of several motor reflexes was also recorded on alternate days (odd days) from PND9 up to PND25. At the end of the treatment period and always just before the last dose or at least 24 h after this last BCP injection (in both cases to avoid the acute effects of these last doses; see details below), mice were subjected to some behavioural tests to detect possible benefits of BCP on motor deficits (computer-aided actimeter), cognitive and emotional impairments (Y-maze and T-maze) and autistic-like traits (social interaction test) developed by Syn1-Cre/Scn1a$^{WT/A1783V}$ mice (Satta et al., 2021). To this end, mice were transferred to the behavior room and acclimated for 1 h before testing to prevent that a novel environment can modify the behavioural response. Tests were carried out in the following order: computer-aided actimeter and T-maze (at PND24 just before the last injection), followed by social interaction test and Y-maze (at PND25 just 24 h after the last injection). All animals were tested during the light cycle at the same time of the day (to 9:00 until 12:00 a.m.) in a room illuminated by a dimly lamp (~50 lux) and each individual mouse was tested no more than twice *per* day. In all cases, the behavioural equipment was cleaned with 70% ethanol before prior to the next task to remove residual odors and any olfactory interference. After behavioural testing at PND25, all mice were euthanized by rapid decapitation and brains were rapidly removed and again fixed for one day at 4 °C in fresh 4% paraformaldehyde prepared in 0.1 M phosphate buffered-saline (PBS), pH 7.4, then cryoprotected by immersion in a 30% sucrose solution for a further day, and finally stored at −80 °C for immunohistochemical analysis. During this experiment, we also recorded animal mortality in Syn1-Cre/Scn1a$^{WT/A1783V}$ and Scn1a$^{WT/WT}$ mice treated with BCP or vehicle.

2.3.1. Analysis of hind-limb grasp reflexes

Hind-limb grasp reflex was measured as an index of grasping ability and motor development (Blaney et al., 2013). Mice were held on their back and both front- or hind-limbs were touched with a thin rod of 1 mm diameter. A score of 1 was assigned if the stimulation caused the hind-limb to grasp, whereas a score of 0 was assigned if no response was reached.

2.3.2. Analysis of hind-limbs clasping reflex

Hind-limbs clasping behavior was recorded to assess dystonia. Mice were suspended by their tail facing downward and the extent of hind-limb position was observed and quantified for 30 s according to the following scale: (i) score = 0 for both hind-limbs consistently splayed outward away from the abdomen with splayed toes; (ii) score = 1 for both hind-limbs partially retracted; and (iii) score = 2 for both hind-limbs entirely retracted and touching the abdomen (adapted from Valdeolivas et al., 2017). Data for each mouse correspond to the average of three trials.

2.3.3. Computer-aided actimeter

Motor activity was analyzed in a computer-aided actimeter (Actitrack, Panlab, Barcelona, Spain) and as published elsewhere (Palomo-Garo et al., 2016). This apparatus consisted of a 45 × 45 cm square arena, with infra-red beams all around, spaced 2.5 cm, coupled to a computerized control unit that automatically analyzes the following parameters: (i) distance run in the actimeter (ambulation); (ii) frequency of vertical activity (rearing); (iii) resting time; (iv) mean velocity spent in ambulation; and (v) time spent in fast movements (>5 cm/s). Measurements were recorded for a period of 15 min.

2.3.4. T-maze test

T-maze test was used to assess spatial and working memory in mice, based on the capacity of rodents to explore new environments. Particularly, it explores their natural tendency to alternate their choice of goal arm and explore new environments (spontaneous alternation, no rewarded). The apparatus was a polyvinyl plastic horizontal maze formed by three arms giving rise to a T-shaped maze. In each trial, the mouse was placed in the start point and allowed to freely choose one goal arm (A or B), and then confined in the chosen arm with the door down for 30 s. After 30 s, the mouse is placed back in the start point and, with doors up, allowed again to freely choose a goal arm. The trial must take 1 min and a half maximum. A score of 1 was assigned if mice chose the opposite arm, whereas a score of 0 was assigned if the same arm was chosen). Normally, 6 trials *per* mouse were performed, thus data

corresponding to the average of all trials (Deacon and Rawlins, 2006).

2.3.5. Y-maze test

The Y-maze is a behavioural test used to measure the spatial working memory in mice based on the capacity of rodents to explore new environments. The apparatus is a polyvinyl plastic horizontal maze formed by 3 arms (40 × 12 × 3 cm) placed at 120° angles to each other and designated as A, B and C. Each animal was placed in the centre of the maze and was allowed to freely explore the three arms. The sequence (i.e., ABCCAB, etc.) and the number of arm entries were recorded during 8 min. The spontaneous alternation performance (SAP), a score of three consecutive different arm entries (ABC, CAB, or BCA), was analyzed. Memory impairments are also evaluated by the frequency of same arm returns (SAR) or alternate arm return (AAR). The alternation percentage was calculated according to the equation follows: % alternation = [(number of alternations)/(total arm entries)] × 100 (Joshi et al., 2014).

2.3.6. Social interaction test

To evaluate social performance, this test was conducted in an open field arena (60 × 30 cm) in which each experimental animal was allowed to freely explore a novel unfamiliar congener of the same sex and of similar weight under dim light. The behavior was recorded for 20 min, and the total time spent by the experimental mouse in nonaggressive social interactions such as sniffing, following or grooming the partner, was monitored, as well as the number of active (Ricceri et al., 2017).

2.4. Immunofluorescence analysis

Fixed brains were sliced in coronal sections of 30 μm thick (containing prefrontal cortex, or hippocampus) in a cryostat (Leica CM3050, Leica, Wetzlar, Germany), collected on antifreeze solution (glycerol/ethylene glycol/PBS; 2:3:5) and stored at −20 °C until used. Sections were mounted on gelatin-coated slides and, once adhered, washed with Tris-buffered saline at pH 7.5. Then, sections were permeabilized with Tris-buffered saline containing 0.2% Triton X-100 for 30 min, and unspecificities were blocked with Tris-buffered saline containing 0.1% Triton X-100 and 2% bovine serum albumin (BSA) for 1 h. After several washes with Tris-buffered saline, sections were incubated overnight at 4 °C with the following primary antibodies: (i) polyclonal rabbit anti-mouse Iba-1 antibody (Wako Chemicals, Richmond, VA, USA) used at 1/500 or (ii) polyclonal rabbit anti-mouse GFAP antibody (Dako Cytomation, Glostrup, Denmark) used at 1/200. After incubation, sections were washed in Tris-buffered saline, followed by incubation for 2 h at 37 °C with the corresponding anti-rabbit secondary antibodies conjugated with Alexa 488 or 546 (Life Technologies, Bleiswijk, The Netherlands) used at 1/200, rendering green or red, respectively, fluorescence. Negative control sections were obtained using the same protocol with omission of the primary antibody. A Leica DMRB microscope and a DFC300FX camera (Leica, Wetzlar, Germany) were used for the observation and photography of the slides, respectively. Immunostaining was quantified by measuring the mean density of labelling in the selected area using the ImageJ software (U.S. National Institutes of Health, Bethesda, Maryland, USA, http://imagej.nih.gov/ij/, 1997–2012). For quantification, high resolution digital microphotographs were taken with the 10× objective under the same conditions of light, brightness and contrast. Data were normalized over the values of wild-type mice.

2.5. Statistical analysis

All data were first analyzed to confirm that they are normally distributed using both the Shapiro-Wilk and the Kolmogorov-Smirnow normality tests, and then were assessed by the two-way (with repeated measures in some cases) ANOVA followed by the Tukey or the Bonferroni test, as required. In those few cases (data in the actimeter and T-maze tests), in which the distribution was not normal, the non-parametric Kruskal-Wallis test followed by Dunn's multiple comparison test was used. All statistical analyses were carried out using GraphPad Prism® software (version 8.0; GraphPad Software Inc., San Diego, CA, USA). Survival data were assessed using Log-Rank test and presented with a Kaplan-Meier analysis. For the two experiments, sample sizes were ≥5 (with very few exceptions indicated in the legends to figures or visible in the scatter plots), always with higher numbers in $Scn1a^{WT/WT}$ mice compared to Syn1-Cre/$Scn1a^{WT/A1783V}$ animals as a consequence of lower breeding outcome (due to possible prenatal mortality) and greater postnatal mortality in DS genotype. In addition, it is important to take into account that, compared to our previous study (Satta et al., 2021), Syn1-Cre/$Scn1a^{WT/A1783V}$ mice were distributed here in three treatment groups in the first experiment and in two groups in the second experiment. This means sample sizes not equivalent to this previous study, but within the standard requirements for a correct statistical assessment.

3. Results

3.1. BCP as an anticonvulsant agent in Syn1-Cre/$Scn1a^{WT/A1783V}$ and $Scn1a^{WT/WT}$ mice

Previous studies have shown that BCP protects against seizures in preclinical models of epilepsy (Liu et al., 2015; de Oliveira et al., 2016; Tchekalarova et al., 2018). In our first approach (acute paradigm), we addressed the anticonvulsant effect of BCP against PTZ-induced seizures in both Syn1-Cre/$Scn1a^{WT/A1783V}$ and $Scn1a^{WT/WT}$ mice. We corroborated that PTZ evokes a more intense seizure-related behavior in Syn1-Cre/$Scn1a^{WT/A1783V}$ mice when compared with the response in $Scn1a^{WT/WT}$ mice (Satta et al., 2021), as indicated by the latencies to myoclonic jerks (genotype: $F(1,52) = 2.53$, $p = 0.117$; see Fig. 1A) and to generalized seizures (genotype: $F(1,50) = 3.36$, $p = 0.07$; see Fig. 1B) as well as the difference between both latencies (genotype: $F(1,43) = 7.88$, $p < 0.001$; see Fig. 1C), which showed numerical trends towards a reduction in Syn1-Cre/$Scn1a^{WT/A1783V}$ mice (treated with vehicle) compared to $Scn1a^{WT/WT}$ mice (treated with vehicle), despite the differences with the post-hoc analysis did not reach statistical significance. The same finding was evident when analyzing the time spent in generalized seizures, which, in this case, was significantly elevated in Syn1-Cre/$Scn1a^{WT/A1783V}$ mice (treated with vehicle) in response to PTZ when compared with the value measured in $Scn1a^{WT/WT}$ mice (treated with vehicle) also in response to PTZ (genotype: $F(1,55) = 3.17$, $p = 0.08$; see Fig. 1D).

The treatment with BCP had no effect on the latency to myoclonic jerks in both Syn1-Cre/$Scn1a^{WT/A1783V}$ and $Scn1a^{WT/WT}$ mice (treatment: $F(1,52) = 0.13$, ns; interaction: $F(1,52) = 1.57$, ns; see Fig. 1A), but tended to elevate the latency to generalized seizures, in particular in $Scn1a^{WT/WT}$ mice (treatment: $F(1,50) = 3.84$, $p = 0.056$; interaction: $F(1,50) = 0.35$, ns; see Fig. 1B). Such beneficial effect was much more evident in the difference between latencies, with the value of time measured in $Scn1a^{WT/WT}$ mice treated with BCP being significantly higher than the same mice treated with vehicle (treatment: $F(1,43) = 4.28$, $p < 0.05$). This was not seen in Syn1-Cre/$Scn1a^{WT/A1783V}$ mice (interaction: $F(1,43) = 2.72$, $p = 0.106$; Fig. 1C). By contrast, the elevated time spent in generalized seizures by Syn1-Cre/$Scn1a^{WT/A1783V}$ mice treated with vehicle was significantly reduced by the treatment with BCP (treatment: $F(1,55) = 14.55$, $p < 0.0005$), a fact also found in $Scn1a^{WT/WT}$ mice but to a much lower extent (interaction: $F(1,55) = 4.49$, $p < 0.05$; Fig. 1D).

Given that: (i) seizuring activity is bidirectionally associated with brain inflammation (Vezzani et al., 2011, 2019), including the case of Syn1-Cre/$Scn1a^{WT/A1783V}$ mice here in which seizures elevated glial reactivity (Satta et al., 2021); and (ii) BCP displays positive effects against neuroinflammatory events and glial reactivity (Gonçalves et al., 2020; Sharma et al., 2016), we investigated the association of astroglial

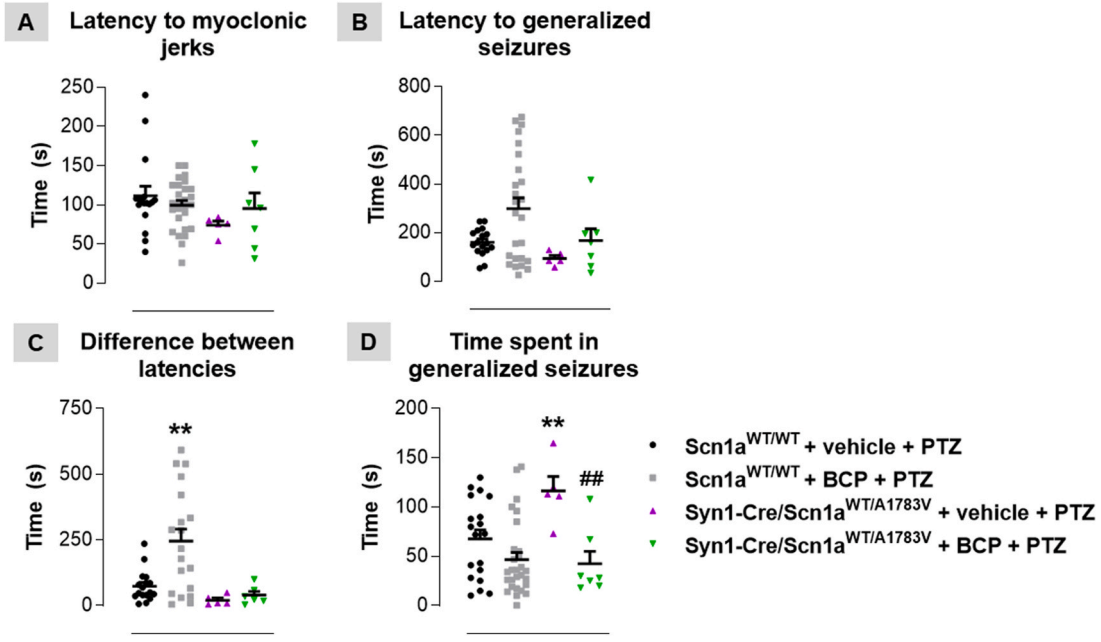

Fig. 1. Effect of an acute treatment with BCP on PTZ-induced seizuring activity in Syn1-Cre/Scn1a$^{WT/A1783V}$ and Scn1a$^{WT/WT}$ mice.
Latency to myoclonic jerks **(A)**, latency to generalized seizures **(B)**, time between generalized seizures and myoclonic jerks **(C)**, and time spent in generalized seizures **(D)** measured in PTZ-treated Syn1-Cre/Scn1a$^{WT/A1783V}$ and Scn1a$^{WT/WT}$ mice at PND25 and after being acutely administered with BCP (100 mg/kg) or vehicle. Values are means ± SEM of ≥5 animals *per* group (see the exact number *per* group in the scatter plots). Data were assessed by two-way (genotype x treatment) ANOVA followed by the Tukey test (**$p < 0.01$ *versus* vehicle-treated Scn1a$^{WT/WT}$ mice and also the remaining groups; $^{\#\#}p < 0.01$ *versus* vehicle-treated Syn1-Cre/Scn1a$^{WT/A1783V}$ mice).

and microglial reactivity in the differences in PTZ-induced seizuring activity in both Syn1-Cre/Scn1a$^{WT/A1783V}$ and Scn1a$^{WT/WT}$ mice, and, in particular, in the benefits provided by the BCP treatment. To this end, we measured GFAP immunofluorescence for astroglial reactivity and Iba-1 immunofluorescence for microglial reactivity in the prefrontal cortex and hippocampal dentate gyrus, the two CNS structures in which we had previously reported that gliosis is more prominent in this DS mouse model (Satta et al., 2021), including in the analysis two additional groups, Syn1-Cre/Scn1a$^{WT/A1783V}$ and Scn1a$^{WT/WT}$ mice in both cases not treated with PTZ, used as controls.

As published previously (Satta et al., 2021), higher levels of GFAP immunostaining were detected in Syn1-Cre/Scn1a$^{WT/A1783V}$ mice compared to Scn1a$^{WT/WT}$ in both the prefrontal cortex (genotype: $F(1, 25) = 529.4$, $p < 0.0001$; see Fig. 2A and B) and the hippocampal dentate gyrus (genotype: $F(1,28) = 15.37$, $p < 0.0005$; see Fig. 2C and D). PTZ elevated the levels of GFAP immunoreactivity compared with mice not treated with PTZ, indicating that this proconvulsant induced reactive astrogliosis (Fig. 2A–D). This induction was apparently equivalent in both genotypes in the prefrontal cortex, assuming that GFAP values were already elevated in Syn1-Cre/Scn1a$^{WT/A1783V}$ before PTZ (Fig. 2A and B). However, a greater PTZ effect was seen in Scn1a$^{WT/WT}$ mice in the hippocampal dentate gyrus (Fig. 2C and D). Lastly, the treatment with BCP reduced also in all cases the elevated levels of GFAP immunostaining, with the greatest reductions in Syn1--Cre/Scn1a$^{WT/A1783V}$ mice instead Scn1a$^{WT/WT}$ animals in the prefrontal cortex (treatment: $F(2,25) = 68.12$, $p < 0.0001$; interaction: $F(2,25) = 16.17$, $p < 0.0001$; see Fig. 2A and B). By contrast, the reductions in GFAP levels caused by BCP in the hippocampal dentate gyrus were more intense in Scn1a$^{WT/WT}$ mice compared to those found in Syn1--Cre/Scn1a$^{WT/A1783V}$ animals (treatment: $F(2,28) = 41.03$, $p < 0.0001$; interaction: $F(2,28) = 4.99$, $p < 0.05$; see Fig. 2C and D).

As expected, elevation of Iba-1 immunoreactivity in the brain of Syn1-Cre/Scn1a$^{WT/A1783V}$ mice compared to Scn1a$^{WT/WT}$ (Satta et al., 2021) was again seen here in the hippocampal dentate gyrus (genotype: $F(1,28) = 13.48$, $p < 0.001$; see Fig. 3C and D), but, to a much lower extent, in the prefrontal cortex (genotype: $F(1,28) = 0.012$, ns; see Fig. 3A and B). Again, the challenge with PTZ elevated in all cases the levels of Iba-1 immunoreactivity compared with mice not treated with this proconvulsant, indicating that PTZ induced reactive microgliosis (Fig. 3A–D). This induction was, in general, more evident in Scn1a$^{WT/WT}$ mice in both the prefrontal cortex and, in particular, in the hippocampal dentate gyrus (Fig. 3A–D). Lastly, the treatment with BCP reduced also in all cases the elevated levels of Iba-1 immunostaining, with the greatest reductions found always in Scn1a$^{WT/WT}$ mice in both the prefrontal cortex (treatment: $F(2,28) = 22.13$, $p < 0.0001$; interaction: $F(2, 28) = 2.61$, $p = 0.092$; see Fig. 3A and B) and the hippocampal dentate gyrus (treatment: $F(2,28) = 85.59$, $p < 0.0001$; interaction: $F(2,28) = 10.71$, $p < 0.0005$; see Fig. 3C and D).

3.2. *BCP as a disease-modifying agent in Syn1-Cre/Scn1a$^{WT/A1783V}$ and Scn1a$^{WT/WT}$ mice*

Once confirmed that BCP was active against seizures in Syn1-Cre/Scn1a$^{WT/A1783V}$ and Scn1a$^{WT/WT}$ mice, in a second experimental approach (repeated treatment), our objective was to evaluate BCP potential as a disease modifier by evaluating its benefits against associated comorbidities in Syn1-Cre/Scn1a$^{WT/A1783V}$ mice (Satta et al., 2021). To this end, we used a repeated treatment with BCP or vehicle in mice of the two genotypes between 10 and 24 days after birth. We first analyzed animal survival in all experimental groups during the whole treatment period. The survival was 100% in vehicle- or BCP-treated Scn1a$^{WT/WT}$ mice at the end of treatment, whereas the survival of vehicle-treated Syn1-Cre/Scn1a$^{WT/A1783V}$ mice drop from PND21 to PND23, resulting in 71.5% of survivors at the end of the experiment (Fig. 4), as expected (Satta et al., 2021). Interestingly, the treatment with BCP slightly improved the survival in Syn1-Cre/Scn1a$^{WT/A1783V}$ mice (75% of survivors) and delayed the occurrence of the first death in two days (up to PND23) compared with those treated with vehicle (Fig. 4). The statistical analysis of these data (progression of survival over the time) indicated they resulted statistically significant ($\chi^2 = 5.061$, $p < 0.05$).

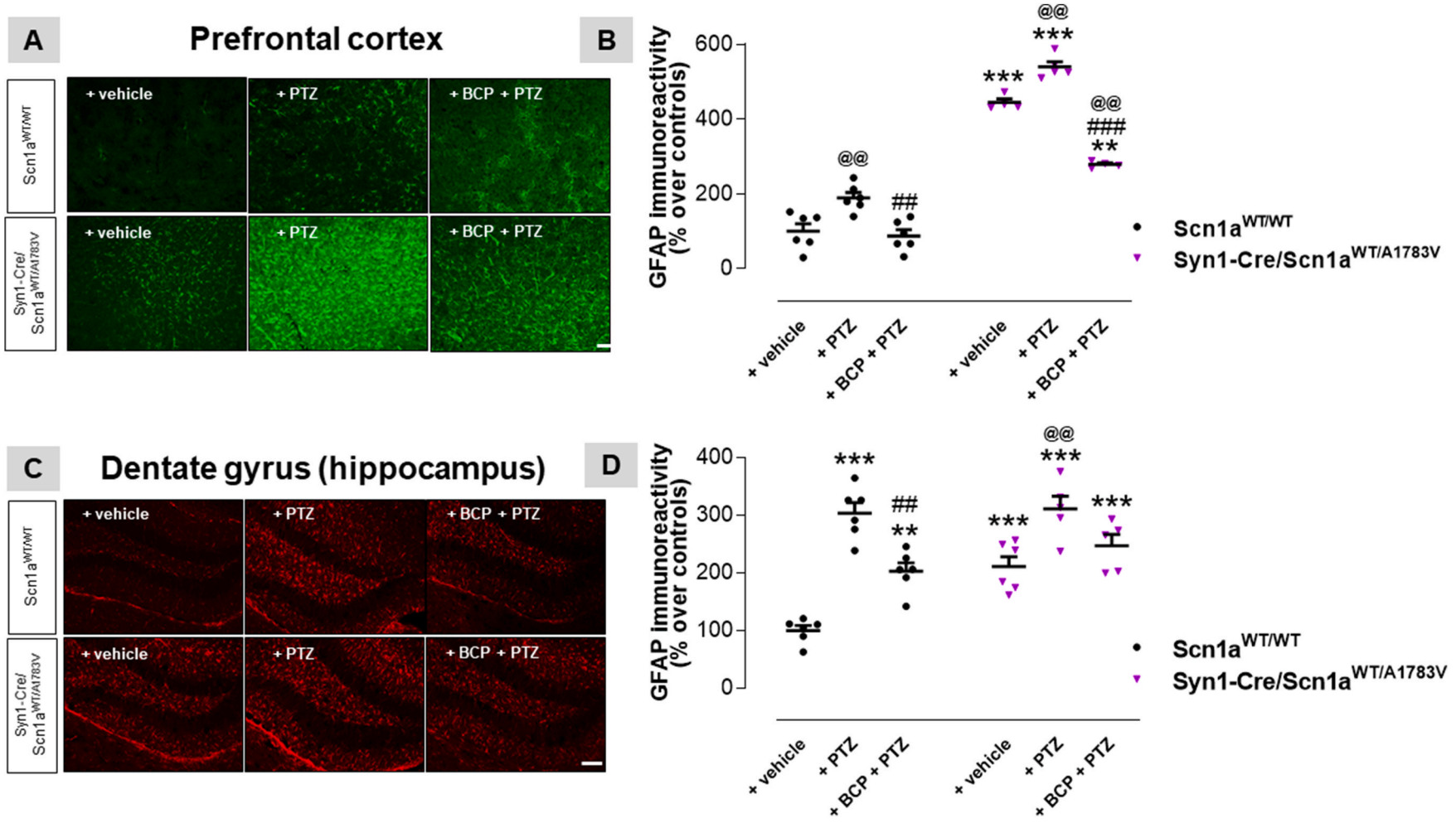

Fig. 2. Effect of an acute treatment with BCP on PTZ-induced reactive astrogliosis in Syn1-Cre/Scn1a$^{WT/A1783V}$ and Scn1a$^{WT/WT}$ mice.
GFAP immunoreactivity in prefrontal cortex **(A** (representative microphotographs) and **B** (quantification)**)** and the hippocampal dentate gyrus **(C** (representative microphotographs) and **D** (quantification)**)** measured in PTZ-treated Syn1-Cre/Scn1a$^{WT/A1783V}$ and Scn1a$^{WT/WT}$ mice at PND25 and after being acutely administered with BCP (100 mg/kg) or vehicle. Groups of Syn1-Cre/Scn1a$^{WT/A1783V}$ and Scn1a$^{WT/WT}$ mice treated with vehicle instead of PTZ were also included as controls. Values are means ± SEM of ≥4 animals *per* group (see the exact number *per* group in the scatter plots). Data were assessed by two-way (genotype x treatment) ANOVA followed by the Tukey test (**$p < 0.01$, ***$p < 0.005$ *versus* vehicle-treated Scn1a$^{WT/WT}$ mice in absence of PTZ challenge (all Scn1a$^{WT/WT}$ mice for GFAP in the prefrontal cortex); $^{@@}p < 0.01$ *versus* vehicle-treated Scn1a$^{WT/WT}$ or Syn1-Cre/Scn1a$^{WT/A1783V}$ mice in absence of PTZ challenge; $^{\#\#}p < 0.01$, $^{\#\#\#}p < 0.005$ *versus* vehicle-treated Scn1a$^{WT/WT}$ or Syn1-Cre/Scn1a$^{WT/A1783V}$ mice after PTZ challenge). Scale bar = 50 μm.

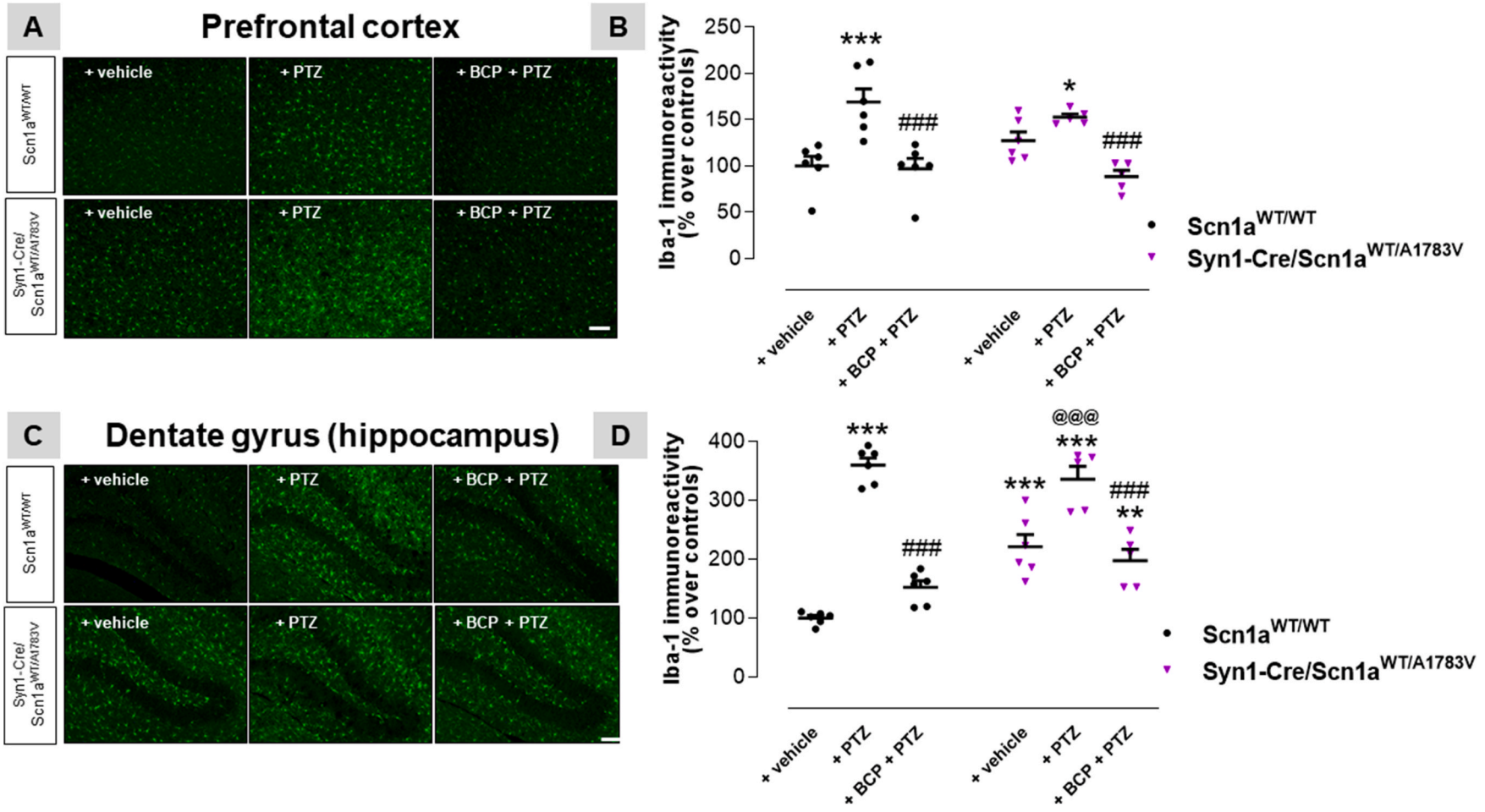

Fig. 3. Effect of an acute treatment with BCP on PTZ-induced reactive microgliosis in Syn1-Cre/Scn1a$^{WT/A1783V}$ and Scn1a$^{WT/WT}$ mice.
Iba-1 immunoreactivity in prefrontal cortex **(A** (representative microphotographs) and **B** (quantification)**)** and the hippocampal dentate gyrus **(C** (representative microphotographs) and **D** (quantification)**)** measured in PTZ-treated Syn1-Cre/Scn1a$^{WT/A1783V}$ and Scn1a$^{WT/WT}$ mice at PND25 and after being acutely administered with BCP (100 mg/kg) or vehicle. Groups of Syn1-Cre/Scn1a$^{WT/A1783V}$ and Scn1a$^{WT/WT}$ mice treated with vehicle instead of PTZ were also included as controls. Values are means ± SEM of ≥5 animals *per* group (see the exact number *per* group in the scatter plots). Data were assessed by two-way (genotype x treatment) ANOVA followed by the Tukey test (*$p < 0.05$, **$p < 0.01$, ***$p < 0.005$ *versus* vehicle-treated Scn1a$^{WT/WT}$ mice in absence of PTZ challenge; $^{@@@}p < 0.005$ *versus* vehicle-treated Syn1-Cre/Scn1a$^{WT/A1783V}$ mice in absence of PTZ challenge; $^{###}p < 0.005$ *versus* the corresponding vehicle-treated Syn1-Cre/Scn1a$^{WT/A1783V}$ or Scn1a$^{WT/WT}$ mice after PTZ challenge). Scale bar = 50 μm.

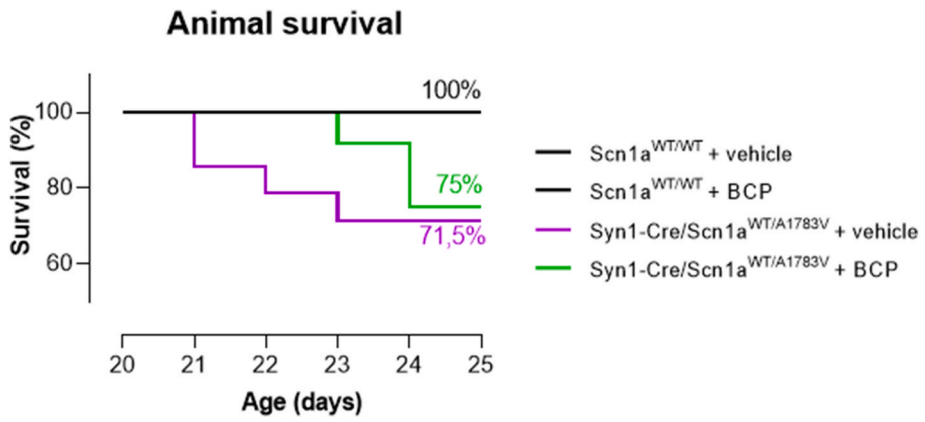

Fig. 4. Effect of a chronic treatment with BCP on animal survival in Syn1-Cre/Scn1a$^{WT/A1783V}$ and Scn1a$^{WT/WT}$ mice.
Kaplan-Meier plot for the analysis of animal survival measured in Syn1-Cre/Scn1a$^{WT/A1783V}$ and Scn1a$^{WT/WT}$ mice chronically treated with BCP (10 mg/kg) or vehicle from PND10 to PND24. Data correspond to 12 animals *per* group and were assessed by Log-Rank test (or Chi-square test).

Weight gain was also recorded in both Syn1-Cre/Scn1a$^{WT/A1783V}$ and Scn1a$^{WT/WT}$ mice repeatedly treated with vehicle or BCP. Our data indicated that vehicle-treated Syn1-Cre/Scn1a$^{WT/A1783V}$ mice experienced a progressive weight loss beginning at PND16 but reaching statistical significance compared to vehicle-treated Scn1a$^{WT/WT}$ mice at PND21 (genotype/treatment: $F(3,32) = 2.24$, $p = 0.103$; time: $F(16,512) = 206.3$, $p < 0.0001$; interaction: $F(48,512) = 2.78$, $p < 0.0001$; see Fig. 5A). Interestingly, the treatment with BCP was able to significantly attenuate this weight loss elevating weight values up to values seen in Scn1a$^{WT/WT}$ mice from PND16 up to PND22, even at higher levels days earlier (Fig. 5A). However, this effect was reduced, losing statistically significance at the last three days analyzed (PND23-25) before sacrifice (Fig. 5A). BCP treatment in Scn1a$^{WT/WT}$ mice did not produce any effects in weight gain (Fig. 5A).

We also investigated the occurrence of some neurodevelopmental anomalies in vehicle-treated Syn1-Cre/Scn1a$^{WT/A1783V}$ mice (Satta

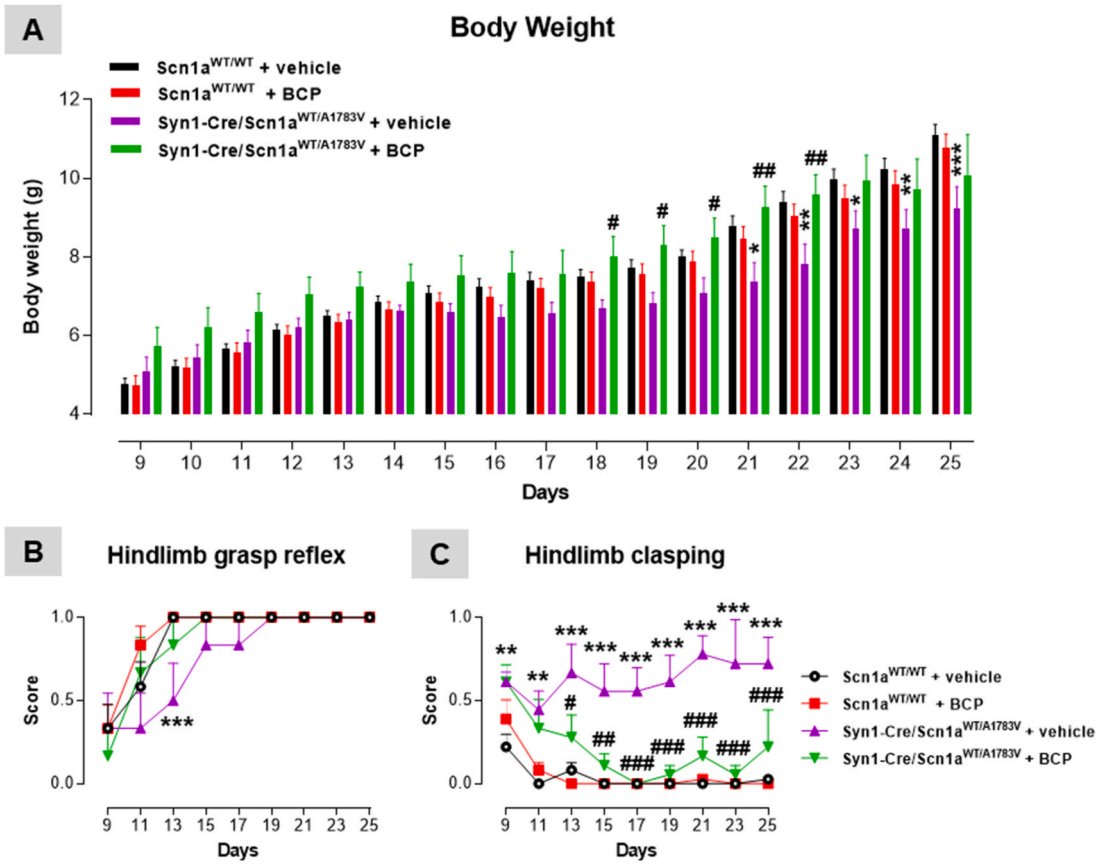

Fig. 5. Effect of a chronic treatment with BCP on the progression of different developmental parameters in Syn1-Cre/Scn1a$^{WT/A1783V}$ and Scn1a$^{WT/WT}$ mice.
Body weight **(A)**, hindlimb grasp reflex **(B)** and hindlimb clasping **(C)** measured in Syn1-Cre/Scn1a$^{WT/A1783V}$ and Scn1a$^{WT/WT}$ mice chronically treated with BCP (10 mg/kg) or vehicle from PND10 to PND24. Values are means ± SEM of 12 animals *per* each Scn1a$^{WT/WT}$ group and 6 *per* each Syn1-Cre/Scn1a$^{WT/A1783V}$ group. Data were assessed by two-way (genotype/treatment x time) ANOVA for repeated measures followed by the Bonferroni test ($^{*}p < 0.05$, $^{**}p < 0.01$, $^{***}p < 0.005$ *versus* vehicle-treated Scn1a$^{WT/WT}$ mice; $^{\#}p < 0.05$, $^{\#\#}p < 0.01$, $^{\#\#\#}p < 0.005$ *versus* vehicle-treated Syn1-Cre/Scn1a$^{WT/A1783V}$ mice).

et al., 2021), in particular the delay in the appearance of hindlimb grasping, which was completely acquired at PND19, so 6 days later compared to Scn1a$^{WT/WT}$ mice, which acquired this reflex at PND13 (genotype/treatment: $F(3,32) = 2.77$, $p = 0.057$; time: $F(8,256) = 31.99$, $p < 0.0001$; interaction: $F(24,256) = 1.28$, $p = 0.178$; see Fig. 5B). Interestingly, the treatment with BCP, which had no effect in Scn1a$^{WT/WT}$ mice, did produce a significant anticipation in the acquirement of this reflex in Syn1-Cre/Scn1a$^{WT/A1783V}$ mice, which occurred at PND15 (Fig. 5B).

Similar results were observed in relation with the hindlimb clasping response, which did not exist (except marginally at PND9) in Scn1a$^{WT/WT}$ mice, but proved a significant elevation at all ages analyzed (from PND9 to PND25) in Syn1-Cre/Scn1a$^{WT/A1783V}$ mice (genotype/treatment: $F(3,32) = 59.10$, $p < 0.0001$; time: $F(8,256) = 6.51$, $p < 0.0001$; interaction: $F(24,256) = 1.67$, $p < 0.05$; see Fig. 5C). The repeated treatment with BCP, which had no effect in Scn1a$^{WT/WT}$ mice, did produce a significant attenuation of this response in Syn1-Cre/Scn1a$^{WT/A1783V}$ mice, which was already visible at PND13 but prolonged for the whole period analyzed, in some cases reaching values similar to Scn1a$^{WT/WT}$ mice (Fig. 5C).

Due to the immaturity of mice, the above parameters were the only that could be recorded during the treatment window (PND10-24). However, the last days of this window, animals were sufficiently mature to be investigated in additional behavioural tests just before being euthanized for analysis of histopathological markers. Thus, we first investigated the response of the two genotypes and the two treatments in a computer-aided actimeter useful to detect motor abnormalities. Our data corroborated, at least in part, the motor hyperactivity described in our previous study in Syn1-Cre/Scn1a$^{WT/A1783V}$ mice (Satta et al., 2021). This was reflected in their longer distance travelled (Kruskal-Wallis: $H(4) = 7.16$, $p = 0.067$), shorter resting time (Kruskal-Wallis: $H(4) = 7.16$, $p = 0.067$), increased average velocity (Kruskal-Wallis: $H(4) = 7.80$, $p = 0.05$), elevated time moving fast (Kruskal-Wallis: $H(4) = 6.65$, $p = 0.084$), and, to a lower extent, more frequent rears (Kruskal-Wallis: $H(4) = 6.65$, $p = 0.09$). However, only the values of resting time and mean velocity were confirmed with the post-hoc test as statistically significant respect Scn1a$^{WT/WT}$ mice treated with vehicle, with the changes in the rest of parameters remaining as mere numerical trends (see Fig. 6A–E). Such increased motor activity was also appreciated in the track plots automatically generated by the Actitrack software (Fig. 6F). The treatment with BCP did not produce any statistically significant effect in both Syn1-Cre/Scn1a$^{WT/A1783V}$ and Scn1a$^{WT/WT}$ mice, but showed a clear trend towards attenuating the hyperactivity found in Syn1-Cre/Scn1a$^{WT/A1783V}$ mice, which was reflected in the loss of statistical significance (or the numerical trends) of Syn1-Cre/Scn1a$^{WT/A1783V}$ mice *versus* Scn1a$^{WT/WT}$ animals (Fig. 6A–E).

Next, we studied the effect of BCP on autism-related behavioural deficits observed in Syn1-Cre/Scn1a$^{WT/A1783V}$ mice in comparison to Scn1a$^{WT/WT}$ animals in the social interaction test (Satta et al., 2021). As expected, Syn1-Cre/Scn1a$^{WT/A1783V}$ mice exhibited a significant decrease in the time spent in active interaction (genotype: $F(1,29) = 16.36$, $p < 0.0005$), as well as in the total number of active interactions (genotype: $F(1,31) = 16.32$, $p < 0.0005$) with a novel unfamiliar partner, in comparison with Scn1a$^{WT/WT}$ mice (Fig. 7A and B). Both deficits were attenuated by BCP administration (Fig. 7A and B), in this case, to a greater extent than in actimeter parameters, despite the differences between BCP- and vehicle-treated Syn1-Cre/Scn1a$^{WT/A1783V}$ mice only reached statistical significance for the total number of active interactions (treatment: $F(1,31) = 5.66$, $p < 0.05$; interaction: $F(1,31) = 6.79$, $p < 0.05$), remaining as a mere numerical trend for the time spent in active interaction (treatment: $F(1,29) = 3.11$, $p = 0.088$; interaction: $F(1,29) = 1.52$, ns). The treatment with BCP in Scn1a$^{WT/WT}$ mice was inactive (Fig. 7A and B).

Lastly, we also explored the effects of BCP against spatial working memory deficits detected in Syn1-Cre/Scn1a$^{WT/A1783V}$ mice (Satta et al., 2021), using both Y-Maze and T-Maze tests. As expected, Syn1-Cre/Scn1a$^{WT/A1783V}$ mice exhibited an impaired performance in the Y-Maze test compared to Scn1a$^{WT/WT}$ mice, with a marked decrease in

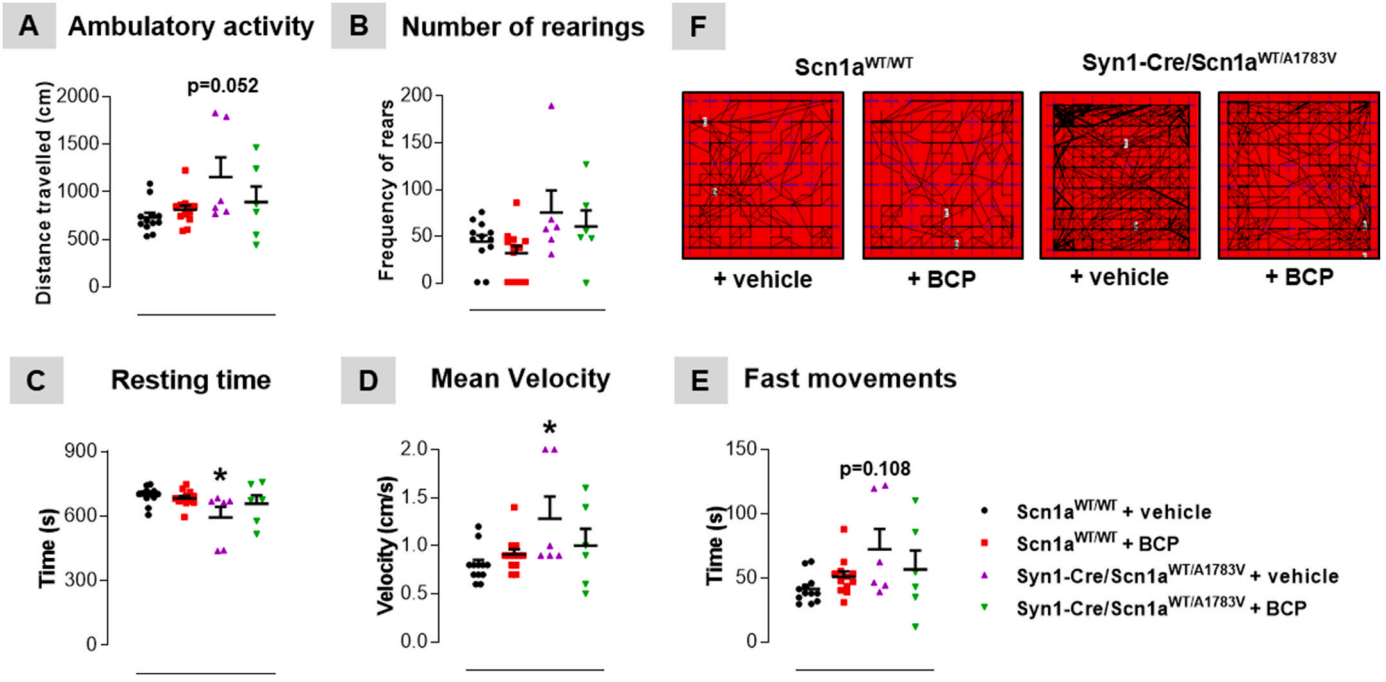

Fig. 6. Effect of a chronic treatment with BCP on the motor activity in Syn1-Cre/Scn1a$^{WT/A1783V}$ and Scn1a$^{WT/WT}$ mice.
Ambulatory activity **(A)**, frequency of rearing behavior **(B)**, resting time **(C)**, mean velocity **(D)**, and time in fast movements **(E)** measured in a computer-aided actimeter in Syn1-Cre/Scn1a$^{WT/A1783V}$ and Scn1a$^{WT/WT}$ mice at PND25 and after being chronically treated with BCP (10 mg/kg) or vehicle from PND10 to PND24. Panel **F** shows some representative track plots generated from the Actitrack software. Values are means ± SEM of ≥5 animals *per* group (see the exact number *per* group in the scatter plots). Data were assessed by Krukal-Wallis test followed by the Dunn's multiple comparison test (*$p < 0.05$ *versus* vehicle-treated Scn1a$^{WT/WT}$ mice).

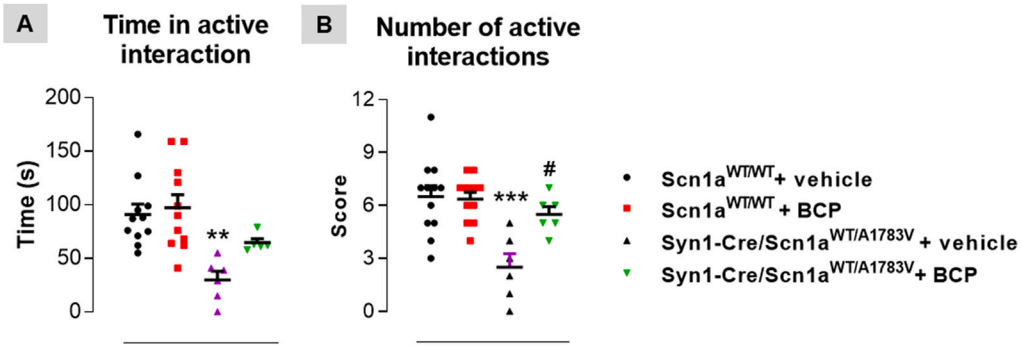

Fig. 7. Effect of a chronic treatment with BCP on the social interaction behavior in Syn1-Cre/Scn1a$^{WT/A1783V}$ and Scn1a$^{WT/WT}$ mice.
Time in active interaction **(A)** and number of active interactions **(B)** measured in the social interaction test in Syn1-Cre/Scn1a$^{WT/A1783V}$ and Scn1a$^{WT/WT}$ mice at PND25 and after being chronically treated with BCP (10 mg/kg) or vehicle from PND10 to PND24. Values are means ± SEM of ≥5 animals *per* group (see the exact number *per* group in the scatter plots). Data were assessed by two-way (genotype x treatment) ANOVA followed by the Tukey test (**p < 0.01, ***p < 0.005 *versus* vehicle-treated Scn1a$^{WT/WT}$ mice).

the spontaneous alternation performance (genotype: $F(1,31) = 11.75$, $p < 0.005$; treatment: $F(1,31) = 0.42$, ns; interaction: $F(1,31) = 4.73$, $p < 0.05$; see Fig. 8B) and small trends towards an increase in the % of alternate arm returns (genotype: $F(1,31) = 8.74$, $p < 0.01$; treatment: $F(1,31) = 0.002$, ns; interaction: $F(1,31) = 0.17$, ns; see Fig. 8C) and in the % of same arm returns (genotype: $F(1,29) = 2.06$, $p = 0.162$; treatment: $F(1,29) = 2.18$, $p = 0.150$; interaction: $F(1,29) = 0.12$, ns; see Fig. 8D). No differences were seen in the number of total entries in the maze arms (genotype: $F(1,30) = 0.24$, ns; treatment: $F(1,30) = 0.20$, ns; interaction: $F(1,30) = 1.75$, ns; see Fig. 8A). The memory impairment exhibited by Syn1-Cre/Scn1a$^{WT/A1783V}$ mice in the Y-Maze test was also evident in the T-Maze task with a significant reduction in the score of these mice in comparison with Scn1a$^{WT/WT}$ animals (Kruskal-Wallis: $H(4) = 12.81$, $p < 0.01$; see Fig. 8E). The treatment with BCP only showed a trend towards an attenuation in Y-Maze deficits, in particular in the spontaneous alternation performance (Fig. 8B) and, to a lower extent, in the number of total entries (Fig. 8A; this effect indirectly supports the efficacy of BCP on motor hyperactivity as shown in the computer-aided actimeter). By contrast, BCP did improve task performance in T-Maze in Syn1-Cre/Scn1a$^{WT/A1783V}$ mice, with no effect in Scn1a$^{WT/WT}$ mice (Fig. 8E).

Most of the aforementioned behavioural abnormalities exhibited by vehicle-treated Syn1-Cre/Scn1a$^{WT/A1783V}$ mice were accompanied by glial reactivity in specific CNS structures. Thus, our data indicated elevated GFAP immunoreactivity both in the prefrontal cortex (genotype: $F(1,20) = 20.37$, $p < 0.0005$; treatment: $F(1,20) = 2.65$, $p = 0.119$; interaction: $F(1,20) = 5.34$, $p < 0.05$; see Fig. 9A and B) and in the hippocampal dentate gyrus (genotype: $F(1,18) = 5.81$, $p < 0.05$;

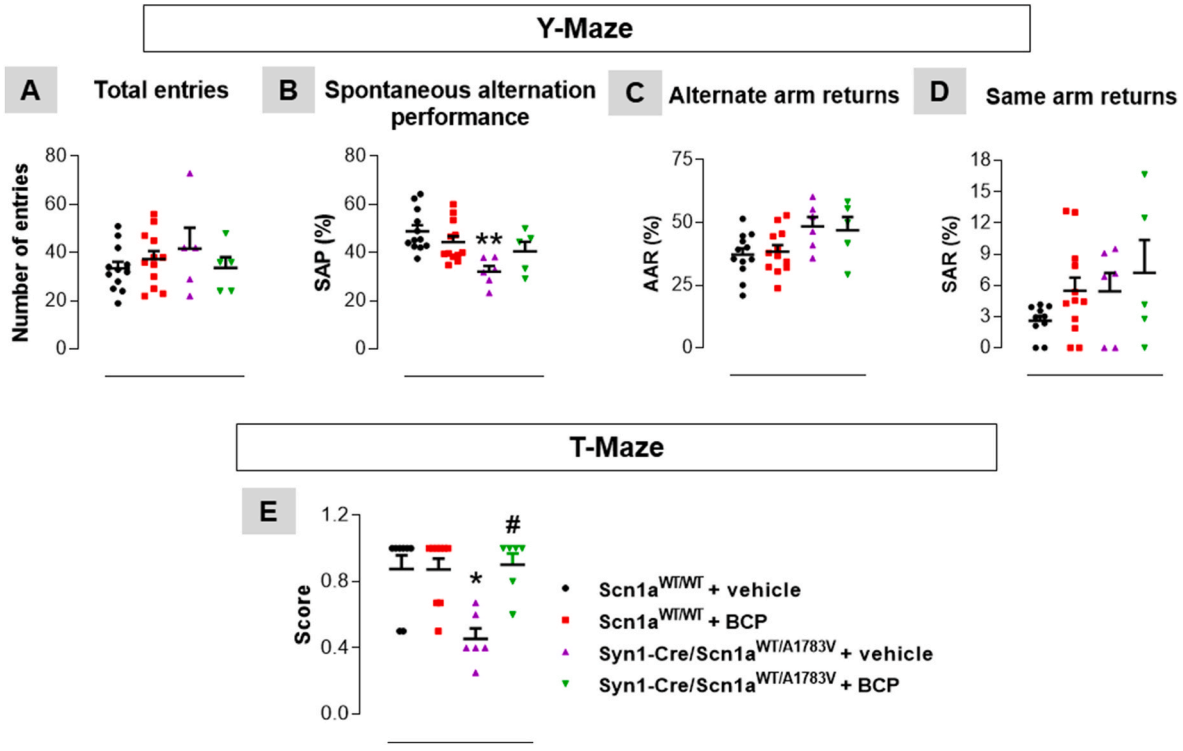

Fig. 8. Effect of a chronic treatment with BCP on the spatial working memory in Syn1-Cre/Scn1a$^{WT/A1783V}$ and Scn1a$^{WT/WT}$ mice.
Number of total entries **(A)**, spontaneous alternation performance **(B)**, alternate arm returns **(C)** and same arm returns **(D)** measure in the Y-Maze test, and score **(E)** measured in the T-Maze test in Syn1-Cre/Scn1a$^{WT/A1783V}$ and Scn1a$^{WT/WT}$ mice at PND25 and after being chronically treated with BCP (10 mg/kg) or vehicle from PND10 to PND24. Values are means ± SEM of ≥5 animals *per* group (see the exact number *per* group in the scatter plots). Y-maze data were assessed by two-way (genotype x treatment) ANOVA followed by the Tukey test, whereas T-maze data were assessed by Krukal-Wallis test followed by the Dunn's multiple comparison test (*p < 0.05, **p < 0.01 *versus* vehicle- and BCP-treated Scn1a$^{WT/WT}$ mice; $^{\#}$p < 0.05 *versus* vehicle-treated Syn1-Cre/Scn1a$^{WT/A1783V}$ mice).

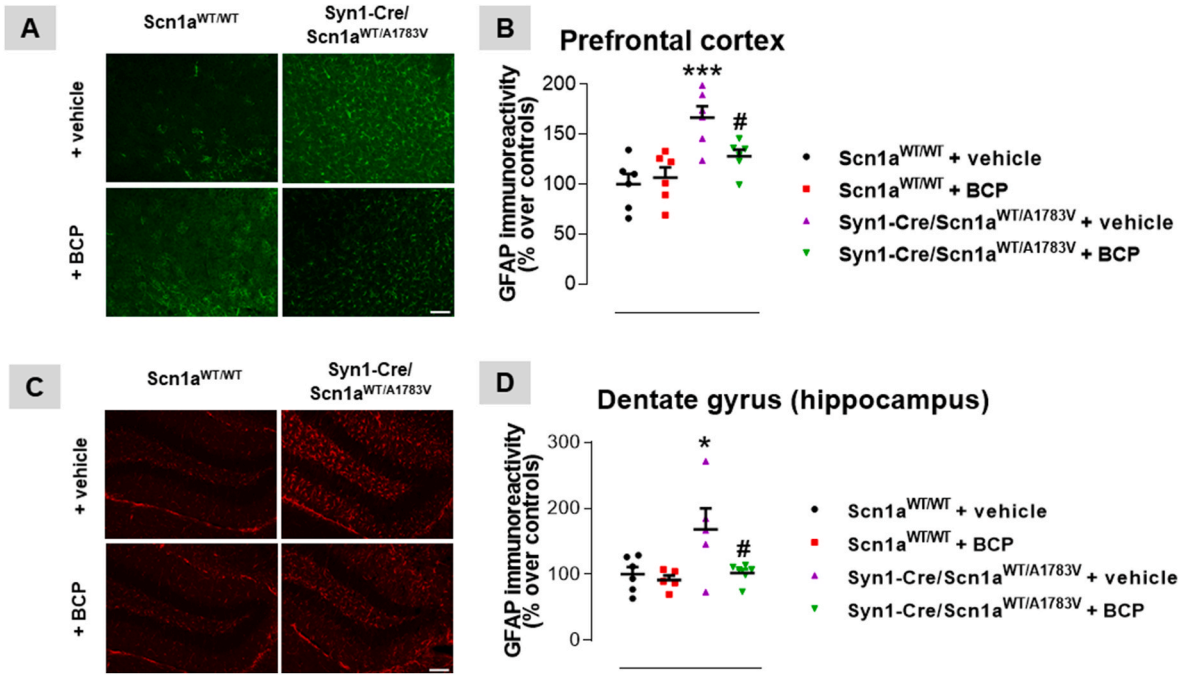

Fig. 9. Effect of a chronic treatment with BCP on reactive astrogliosis in Syn1-Cre/Scn1a$^{WT/A1783V}$ and Scn1a$^{WT/WT}$ mice.
GFAP immunoreactivity in prefrontal cortex **(A** (representative microphotographs) and **B** (quantification)**)** and the hippocampal dentate gyrus **(C** (representative microphotographs) and **D** (quantification)**)** measured in Syn1-Cre/Scn1a$^{WT/A1783V}$ and Scn1a$^{WT/WT}$ mice at PND25 and after being chronically treated with BCP (10 mg/kg) or vehicle from PND10 to PND24. Values are means ± SEM of ≥5 animals *per* group (see the exact number *per* group in the scatter plots). Data were assessed by two-way (genotype x treatment) ANOVA followed by the Tukey test (*$p < 0.05$, ***$p < 0.005$ *versus* Scn1a$^{WT/WT}$ mice; $^{\#}p < 0.05$ *versus* vehicle-treated Syn1-Cre/Scn1a$^{WT/A1783V}$ mice). Scale bar = 50 μm.

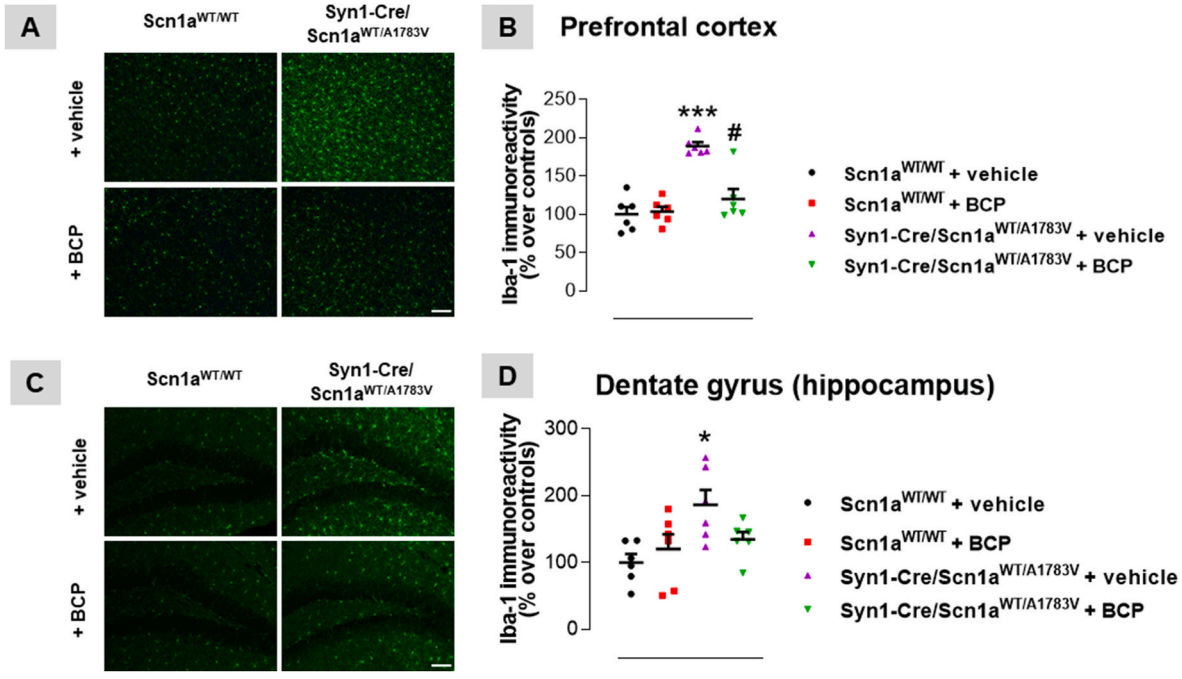

Fig. 10. Effect of a chronic treatment with BCP on reactive microgliosis in Syn1-Cre/Scn1a$^{WT/A1783V}$ and Scn1a$^{WT/WT}$ mice.
Iba-1 immunoreactivity in prefrontal cortex **(A** (representative microphotographs) and **B** (quantification)**)** and the hippocampal dentate gyrus **(C** (representative microphotographs) and **D** (quantification)**)** measured in Syn1-Cre/Scn1a$^{WT/A1783V}$ and Scn1a$^{WT/WT}$ mice at PND25 and after being chronically treated with BCP (10 mg/kg) or vehicle from PND10 to PND24. Values are means ± SEM of ≥5 animals *per* group (see the exact number *per* group in the scatter plots). Data were assessed by two-way (genotype x treatment) ANOVA followed by the Tukey test (*$p < 0.05$, ***$p < 0.005$ *versus* Scn1a$^{WT/WT}$ mice; $^{\#}p < 0.05$ *versus* vehicle-treated Syn1-Cre/Scn1a$^{WT/A1783V}$ mice). Scale bar = 50 μm.

treatment: $F(1,18) = 5.29$, $p < 0.05$; interaction: $F(1,18) = 3.12$, $p = 0.09$; Fig. 9C and D) in Syn1-Cre/Scn1a$^{WT/A1783V}$ mice in comparison with Scn1a$^{WT/WT}$ mice. A similar elevation was also evident for Iba-1 immunoreactivity again in the prefrontal cortex (genotype: $F(1,20) = 35.02$, $p < 0.0001$; treatment: $F(1,20) = 13.70$, $p < 0.005$; interaction: $F(1,20) = 16.53$, $p < 0.001$; see Fig. 10A and B) and, to a lesser extent, in the hippocampal dentate gyrus (genotype: $F(1,20) = 8.01$, $p < 0.05$; treatment: $F(1,20) = 0.78$, ns; interaction: $F(1,20) = 4.06$, $p = 0.058$; see Fig. 10C and D). The repeated administration of BCP was highly active in Syn1-Cre/Scn1a$^{WT/A1783V}$ mice against these astroglial and microglial reactivities with effects that strongly attenuated the elevated GFAP (Fig. 9A–D) or Iba-1 (Fig. 10A–D) immunoreactivities in both CNS structures, reaching, in general, statistical significance respect the vehicle-treated Syn1-Cre/Scn1a$^{WT/A1783V}$ mice, except in the case of Iba-1 in the hippocampal dentate gyrus which remains as a potent trend (Fig. 10B).

4. Discussion

Recent experimental evidence obtained in preclinical and clinical studies have situated cannabinoids, in particular CBD, as a promising agent for the treatment of DS and other related infantile refractory epileptic syndromes (Devinsky et al., 2017, 2019, 2019; Kaplan et al., 2017; Thiele et al., 2018, 2019; Miller et al., 2020; Patra et al., 2020). Such potential may be also evident for cannabinoids other than CBD, which may have a similar broad-spectrum profile. This may be the case of BCP, a sesquiterpene abundantly found in different plants including *Cannabis Sativa* (Sharma et al., 2016; Gonçalves et al., 2020). As mentioned in the Introduction, BCP was first described as a full and selective agonist of CB_2 receptors (Gertsch et al., 2008), but further studies have demonstrated that it is also able to act on numerous receptors and other pharmacological targets (Sharma et al., 2016). Such multitarget profile allows BCP, as happens with CBD, to exert numerous pharmacological effects, including antioxidant, anti-inflammatory, anticonvulsant, antinociceptive and neuroprotective properties, among others (Sharma et al., 2016; Hashiesh et al., 2021). In addition, as happens with CBD, BCP is non-psychoactive as it has no activity at the CB_1 receptor (Hashiesh et al., 2021). This situates BCP as a promising cannabinoid candidate for a wide variety of therapeutic applications (Sharma et al., 2016; Gonçalves et al., 2020; Hashiesh et al., 2021), including cerebral ischemia, neurodegenerative pathologies, neuropathic pain and other CNS-related pathological conditions, but also liver fibrosis, atherosclerosis, nephrotoxicity and other peripheral pathologies (Hashiesh et al., 2021).

In the present study, we have investigated BCP as a useful therapeutic agent in DS, using an experimental model of this disease which we have recently characterized for studies with cannabinoid compounds (Satta et al., 2021). The study was concentrated on two therapeutic benefits, on one hand, the capability of BCP to have antiseizuring activity in DS. This capability has been previously investigated in different animal models of epilepsy (e.g., models based on PTZ- or kainate-induced seizures), but not in DS, and has been related to its ability to attenuate inflammatory events which are typically linked to hyperexcitability (Liu et al., 2015; de Oliveira et al., 2016; Tchekalarova et al., 2018). Our data have corroborated the antiseizuring potential of BCP which attenuated the proconvulsant action of PTZ, with this potential being found in Syn1-Cre/Scn1a$^{WT/A1783V}$ mice but also in their controls (Scn1a$^{WT/WT}$) mice. Our data also corroborates that these beneficial effects against PTZ-induced seizuring responses were paralleled by a reduction in astroglial (labelled with GFAP) and microglial (labelled with Iba-1) reactivities induced by the PTZ challenge in both genotypes (analyzed in the medial prefrontal cortex and the hippocampal dentate gyrus). It is important to remark that these benefits, at both behavioural (against proconvulsant activity) and inflammatory (against glial reactivity) levels, caused by BCP occurred always in both genotypes and were, in general, of relatively equivalent magnitude, although we confirmed the existence of some important differences between Syn1-Cre/Scn1a$^{WT/A1783V}$ and Scn1a$^{WT/WT}$ mice (e.g. elevated glial reactivity in DS mice), already described (Satta et al., 2021), but that affect, in general, to the values in absence of PTZ challenge.

We were also interested in investigating, as a second approach, whether BCP, in a longer treatment (from PND10 up to PND24), may be also active against several long-term comorbidities associated with DS, which have been identified in patients (Dravet, 2011) and also in this (Satta et al., 2021) and other experimental models of this disease (reviewed in Griffin et al., 2018). BCP corrected important behavioural abnormalities found in Syn-Cre/Scn1a$^{WT/A1783V}$ mice, such as the delay in the appearance of hindlimb grasp reflex, the induction of clasping response, a certain motor hyperactivity, the altered social interaction, and the memory impairment, which represent important comorbidities found in experimental DS (reviewed in Griffin et al., 2018). The treatment with BCP also attenuated the loss of weight experienced by Syn--Cre/Scn1a$^{WT/A1783V}$ mice, and had a small but relevant effect in delaying the premature mortality (before PND25) detected for these mice. We assume that these behavioural effects (and also those on attenuating glial reactivity that will be described below) are not a transient and reversible effect caused acutely by the dose administered prior to behavioural testing, as this injection was carried out 24 h before, time sufficient for an important clearance of BCP according to previous pharmacokinetic studies with this compound (Liu et al., 2013). We believe that these effects are more related to the disease-modifying properties of BCP exerted in repeated treatments and that allow this compound, as happens with CBD, to prevent or to attenuate the occurrence of long-term comorbidities, based on its antioxidant, anti-inflammatory, anticonvulsant, antinociceptive and neuroprotective properties (Sharma et al., 2016; Gonçalves et al., 2020; Hashiesh et al., 2021).

We were also interested in exploring whether effects of BCP in attenuating glial reactivity and associated inflammatory events occurring in the CNS, in particular in those structures more involved in the behavioural abnormalities detected in these mice, such as the medial prefrontal cortex and the hippocampal dentate gyrus, may be associated with its behavioural benefits. This hypothesis was based on previous results described in other epileptic conditions (Liu et al., 2015), as well as in normal brain aging (Chávez-Hurtado et al., 2020) and in different neurodegenerative disorders, e.g., Alzheimer's disease (Cheng et al., 2014), Parkinson's disease (Viveros-Paredes et al., 2017), stroke (Tian et al., 2019). Our data point in this direction as the repeated treatment with BCP in Syn-Cre/Scn1a$^{WT/A1783V}$ mice strongly reduced the reactive astrogliosis (labelled with GFAP) and microgliosis (labelled with Iba-1) in the two areas under investigation, without having any effect in Scn1a$^{WT/WT}$ mice, in which BCP had not altered any of the behavioural parameters analyzed. Anyway, to establish definitively a cause-effect relationship between the anti-inflammatory effects of BCP and its behavioural improvements will require further research.

A curious aspect of the data generated in these two experimental approaches is that a high dose of BCP (100 mg/kg) is required to protect against seizures, whereas a much lower dose (10 mg/kg) is enough to improve behavioural disturbances. Although we did not perform *in vivo* dose-response curves, these dosages were defined according to previous studies using BCP (de Oliveira et al., 2016; Viveros-Paredes et al., 2017; Hernández-León et al., 2020). This discrepancy between a high dose required for seizure prevention and a lower dose necessary for improved behavioural outcome is similarly found in studies using CBD (Kaplan et al., 2017) or clonazepam (Han et al., 2012, 2014) in other DS mouse models. This fact could represent a conundrum for defining an appropriate pharmacological approach that both attenuates seizures and long-term outcome. However, in the case of BCP, this issue would be less relevant, since safety of BCP at high doses appears to be well-demonstrated (Sharma et al., 2016). We plan to explore doses higher than 10 mg/kg against long-term comorbidities in future studies with the purpose to get more powerful effects, although it is important to

take into account that using different doses could involve different mechanisms of action. Such optimization could be also reached by exploring possible synergies between BCP and CBD, given that both cannabinoids likely modulate different molecular targets but sharing common effects (e.g. anti-inflammatory, antioxidant) (Russo, 2011). We have preliminary data that this combination is highly effective (Alonso et al., unpublished results).

Although we have not investigated the specific molecular targets that may explain BCP effects in this DS mouse model, it is well established that BCP elicits a full agonist action over CB_2 receptor (Gertsch et al., 2008). In fact, available data suggest that BCP exerts is anti-inflammatory and antioxidant effects through multiple mechanisms normally initiated by the activation of this receptor (Sharma et al., 2016; Machado et al., 2018). Importantly, the lack of psychoactivity associated with CB_2 receptor activation offers BCP a great suitability for pharmaceutical development. Given that protein levels of CB_2 receptor are enhanced in the hippocampus of our DS mice (Satta et al., 2021), we hypothesize that CB_2 receptor may mediate BCP therapeutic action. In agreement with this possibility, CB_2 receptor is also upregulated in lymphocytes from DS patients (Rubio et al., 2016), which further supports the role of this receptor in this disorder. In addition, some studies have demonstrated BCP activation of PPARs (Sharma et al., 2016). However, direct binding of BCP has been reported only for PPAR-α (Wu et al., 2014), whereas PPAR-γ activation depends on the binding of BCP to CB_2 receptors (O'Sullivan, 2016). Particularly, stimulation of CB_2 receptor by BCP promotes an intracellular signalling cascade, which augments MAP kinase activity that further activates PPAR-γ via direct phosphorylation (O'Sullivan, 2016). In this way, the cross-talk between CB_2 and PPAR-γ receptors may also contribute to activate anti-inflammatory signals (Youssef et al., 2019; Picciolo et al., 2020).

Therefore, our data support that BCP was active in Syn-Cre/$Scn1a^{WT/A1783V}$ mice against seizuring activity in an acute treatment and against several comorbidities after a repeated treatment, in both cases in association with its capability to reduce glial reactivity in areas related to these behavioural abnormalities. This situates BCP in a promising position for further preclinical evaluation towards a close translation to DS patients. In addition, these beneficial effects add to the previous evidence collected for other phytocannabinoid, CBD, which is already approved for the treatment of seizures in DS (Franco et al., 2021) and is being investigated at the preclinical level as a disease modifier (Kaplan et al., 2017; Patra et al., 2020). Our data add BCP as an additional strategy, for which there is also evidence supporting that, under certain circumstances, BCP can act synergistically with CBD and potentiate its effects as a consequence of the so-called "entourage effect'' (Russo, 2011). If confirmed, the combination of both compounds could represent a promising strategy in order to improve the therapeutic management of DS patients.

Ethics statement

The animal study was reviewed and approved by Animal Welfare of the Complutense University (PROEX 033/17).

Funding

This work was supported by grants from CIBERNED (CB06/05/0089) and MICIU (RTI2018-098885-B-100) to JF-R, and "Proyectos de Investigación en Salud, Instituto de Salud Carlos III" (PI20/00773), and Mehuer and CajaSol foundations to OS. These agencies had no further role in study design, collection, analysis and interpretation of the data, in the writing of the report, or in the decision to submit the paper for publication. CA is a predoctoral fellow supported by the FPU-Program (FPU16/04768). The authors are indebted to Yolanda García-Movellán for administrative assistance and to CAI-Animalario, Complutense University for animal housing and care.

CRediT authorship contribution statement

Cristina Alonso: Methodology, Validation, Formal analysis, Investigation, Visualization, Writing – review & editing. **Valentina Satta:** Methodology, Validation, Investigation, Writing – review & editing. **Paula Díez-Gutiérrez:** Investigation, Writing – review & editing. **Javier Fernández-Ruiz:** Conceptualization, Formal analysis, Data curation, Visualization, Supervision, Project administration, Funding acquisition, Writing – original draft, Writing – review & editing. **Onintza Sagredo:** Conceptualization, Formal analysis, Visualization, Supervision, Project administration, Funding acquisition, Writing – review & editing.

Declaration of competing interest

The authors declare that the research was conducted in the absence of any commercial or financial relationships that could be construed as a potential conflict of interest.

References

Alachkar, A., Ojha, S.K., Sadeq, A., Adem, A., Frank, A., Stark, H., Sadek, B., 2020. Experimental models for the discovery of novel anticonvulsant drugs: focus on pentylenetetrazole-induced seizures and associated memory deficits. Curr. Pharmaceut. Des. 26, 1693–1711.

Anderson, L.L., Low, I.K., Banister, S.D., McGregor, I.S., Arnold, J.C., 2019. Pharmacokinetics of phytocannabinoid acids and anticonvulsant effect of cannabidiolic acid in a mouse model of Dravet syndrome. J. Nat. Prod. 82, 3047–3055.

Bender, A.C., Morse, R.P., Scott, R.C., Holmes, G.L., Lenck-Santini, P.P., 2012. SCN1A mutations in Dravet syndrome: impact of interneuron dysfunction on neural networks and cognitive outcome. Epilepsy Behav. 23, 177–186.

Blaney, C.E., Gunn, R.K., Stover, K.R., Brown, R.E., 2013. Maternal genotype influences behavioral development of 3×Tg-AD mouse pups. Behav. Brain Res. 252, 40–48.

Chávez-Hurtado, P., González-Castañeda, R.E., Beas-Zarate, C., Flores-Soto, M.E., Viveros-Paredes, J.M., 2020. β-Caryophyllene reduces DNA oxidation and the overexpression of glial fibrillary acidic protein in the prefrontal cortex and hippocampus of D-galactose-induced aged BALB/c mice. J. Med. Food 23, 515–522.

Cheng, Y., Dong, Z., Liu, S., 2014. β-Caryophyllene ameliorates the Alzheimer-like phenotype in APP/PS1 Mice through CB2 receptor activation and the PPARγ pathway. Pharmacology 94, 1–12.

da Fonsêca, D.V., da Silva Maia Bezerra Filho, C., Lima, T.C., de Almeida, R.N., de Sousa, D.P., 2019. Anticonvulsant essential oils and their relationship with oxidative stress in epilepsy. Biomolecules 9, 835.

de Oliveira, C.C., de Oliveira, C.V., Grigoletto, J., Ribeiro, L.R., Funck, V.R., Grauncke, A. C., de Souza, T.L., Souto, N.S., Furian, A.F., Menezes, I.R., Oliveira, M.S., 2016. Anticonvulsant activity of β-caryophyllene against pentylenetetrazol-induced seizures. Epilepsy Behav. 56, 26–31.

Deacon, R.M.J., Rawlins, N.P., 2006. T-maze alternation in the rodent. Nat. Protoc. 1, 7–12.

Devinsky, O., Marsh, E., Friedman, D., Thiele, E., Laux, L., Sullivan, J., Miller, I., Flamini, R., Wilfong, A., Filloux, F., Wong, M., Tilton, N., Bruno, P., Bluvstein, J., Hedlund, J., Kamens, R., Maclean, J., Nangia, S., Singhal, N.S., Wilson, C.A., Patel, A., Cilio, M.R., 2016. Cannabidiol in patients with treatment-resistant epilepsy: an open-label interventional trial. Lancet Neurol. 15, 270–278.

Devinsky, O., Cross, J.H., Laux, L., Marsh, E., Miller, I., Nabbout, R., Scheffer, I.E., Thiele, E.A., Wright, S., 2017. Trial of cannabidiol for drug-resistant seizures in the Dravet syndrome. N. Engl. J. Med. 376, 2011–2020.

Devinsky, O., Nabbout, R., Miller, I., Laux, L., Zolnowska, M., Wright, S., Roberts, C., 2019. Long-term cannabidiol treatment in patients with Dravet syndrome: an open-label extension trial. Epilepsia 60, 294–302.

Dravet, C., 2011. The core Dravet syndrome phenotype. Epilepsia 52, 3–9.

Fernández-Ruiz, J., Sagredo, O., Pazos, M.R., García, C., Pertwee, R., Mechoulam, R., Martínez-Orgado, J., 2013. Cannabidiol for neurodegenerative disorders: important new clinical applications for this phytocannabinoid? Br. J. Clin. Pharmacol. 75, 323–333.

Franco, V., Bialer, M., Perucca, E., 2021. Cannabidiol in the treatment of epilepsy: current evidence and perspectives for further research. Neuropharmacology 185, 108442.

Gataullina, S., Dulac, O., 2017. From genotype to phenotype in Dravet disease. Seizure 44, 58–64.

Gertsch, J., Leonti, M., Raduner, S., Racz, I., Chen, J.Z., Xie, X.Q., Altmann, K.H., Karsak, M., Zimmer, A., 2008. Beta-caryophyllene is a dietary cannabinoid. Proc. Natl. Acad. Sci. U.S.A. 105, 9099–9104.

Gonçalves, E.C.D., Baldasso, G.M., Bicca, M.A., Paes, R.S., Capasso, R., Dutra, R.C., 2020. Terpenoids, cannabimimetic ligands, beyond the cannabis plant. Molecules 25, 1567.

Gray, R.A., Stott, C.G., Jones, N.A., Di Marzo, V., Whalley, B.J., 2020. Anticonvulsive properties of cannabidiol in a model of generalized seizure are transient receptor potential vanilloid 1 dependent. Cannabis Cannabinoid Res. 5, 145–149.

Griffin, A., Hamling, K.R., Hong, S., Anvar, M., Lee, L.P., Baraban, S.C., 2018. Preclinical animal models for Dravet syndrome: seizure phenotypes, comorbidities and drug screening. Front. Pharmacol. 9, 573.
Han, S., Tai, C., Westenbroek, R.E., Yu, F.H., Cheah, C.S., Potter, G.B., Rubenstein, J.L., Scheuer, T., de la Iglesia, H.O., Catterall, W.A., 2012. Autistic-like behaviour in Scn1a$^{+/-}$ mice and rescue by enhanced GABA-mediated neurotransmission. Nature 489, 385–390.
Han, S., Tai, C., Jones, C.J., Scheuer, T., Catterall, W.A., 2014. Enhancement of inhibitory neurotransmission by GABA-A receptors having α2,3-subunits ameliorates behavioral deficits in a mouse model of autism. Neuron 81, 1282–1289.
Hashiesh, H.M., Sharma, C., Goyal, S.N., Sadek, B., Jha, N.K., Kaabi, J.A., Ojha, S., 2021. A focused review on CB2 receptor-selective pharmacological properties and therapeutic potential of β-caryophyllene, a dietary cannabinoid. Biomed. Pharmacother. 140, 111639.
Hernández-León, A., González-Trujano, M.E., Narváez-González, F., Pérez-Ortega, G., Rivero-Cruz, F., Aguilar, M.I., 2020. Role of β-caryophyllene in the antinociceptive and anti-inflammatory effects of *Tagetes lucida* Cav. essential oil. Molecules 25, 675.
Joshi, R., Garabadu, D., Teja, G.R., Krishnamurthy, S., 2014. Silibinin ameliorates LPS-induced memory deficits in experimental animals. Neurobiol. Learn. Mem. 116, 117–131.
Kaplan, J.S., Stella, N., Catterall, W.A., Westenbroek, R.E., 2017. Cannabidiol attenuates seizures and social deficits in a mouse model of Dravet syndrome. Proc. Natl. Acad. Sci. U.S.A. 114, 11229–11234.
Lagae, L., Brambilla, I., Mingorance, A., Gibson, E., Battersby, A., 2018. Quality of life and comorbidities associated with Dravet syndrome severity: a multinational cohort survey. Dev. Med. Child Neurol. 60, 63–72.
Liu, H., Yang, G., Tang, Y., Cao, D., Qi, T., Qi, Y., Fan, G., 2013. Physicochemical characterization and pharmacokinetics evaluation of β-caryophyllene/β-cyclodextrin inclusion complex. Int. J. Pharm. 450, 304–310.
Liu, H., Song, Z., Liao, D., Zhang, T., Liu, F., Zhuang, K., Luo, K., Yang, L., 2015. Neuroprotective effects of trans-caryophyllene against kainic acid induced seizure activity and oxidative stress in mice. Neurochem. Res. 40, 118–123.
Machado, K.D.C., Islam, M.T., Ali, E.S., Rouf, R., Uddin, S.J., Dev, S., Shilpi, J.A., Shill, M.C., Reza, H.M., Das, A.K., Shaw, S., Mubarak, M.S., Mishra, S.K., Melo-Cavalcante, A.A.C., 2018. A systematic review on the neuroprotective perspectives of beta-caryophyllene. Phytother Res. 32, 2376–2388.
Marini, C., Scheffer, I.E., Nabbout, R., Suls, A., De Jonghe, P., Zara, F., Guerrini, R., 2011. The genetics of Dravet syndrome. Epilepsia 52, 24–29.
Miller, I., Scheffer, I.E., Gunning, B., Sanchez-Carpintero, R., Gil-Nagel, A., Perry, M.S., Saneto, R.P., Checketts, D., Dunayevich, E., Knappertz, V., GWPCARE2 Study Group, 2020. Dose-ranging effect of adjunctive oral cannabidiol vs placebo on convulsive seizure frequency in Dravet syndrome: a randomized clinical rrial. JAMA Neurol 77, 613–621.
O'Sullivan, S.E., 2016. An update on PPAR activation by cannabinoids. Br. J. Pharmacol. 173, 1899–1910.
Palomo-Garo, C., Gómez-Gálvez, Y., García, C., Fernández-Ruiz, J., 2016. Targeting the cannabinoid CB2 receptor to attenuate the progression of motor deficits in LRRK2-transgenic mice. Pharmacol. Res. 110, 181–192.
Patra, P.H., Serafeimidou-Pouliou, E., Bazelot, M., Whalley, B.J., Williams, C.M., McNeish, A.J., 2020. Cannabidiol improves survival and behavioural co-morbidities of Dravet syndrome in mice. Br. J. Pharmacol. 177, 2779–2792.
Perucca, E., 2017. Cannabinoids in the treatment of epilepsy: hard evidence at last? J. Epilepsy Res. 7, 61–76.
Picciolo, G., Pallio, G., Altavilla, D., Vaccaro, M., Oteri, G., Irrera, N., Squadrito, F., 2020. β-Caryophyllene reduces the inflammatory phenotype of periodontal cells by targeting CB2 receptors. Biomedicines 8, 164.
Porter, B.E., Jacobson, C., 2013. Report of a parent survey of cannabidiol-enriched cannabis use in pediatric treatment-resistant epilepsy. Epilepy Behav 29, 574–577.
Ricceri, L., Michetti, C., Scattoni, M.L., 2017. Mouse behavior and models for autism spectrum disorders. In: Neuronal and Synaptic Dysfunction in Autism Spectrum Disorder and Intellectual Disability, pp. 269–293 (chapter 7).
Rosenberg, E.C., Tsien, R.W., Whalley, B.J., Devinsky, O., 2015. Cannabinoids and epilepsy. Neurotherapeutics 12, 747–768.
Rubio, M., Valdeolivas, S., Piscitelli, F., Verde, R., Satta, V., Barroso, E., Montolio, M., Aras, L.M., Di Marzo, V., Sagredo, O., Fernández-Ruiz, J., 2016. Analysis of endocannabinoid signaling elements and related proteins in lymphocytes of patients with Dravet syndrome. Pharmacol. Res. Perspect. 4, e00220.
Russo, E.B., 2011. Taming THC: potential cannabis synergy and phytocannabinoid-terpenoid entourage effects. Br. J. Pharmacol. 163, 1344–1364.
Satta, V., Alonso, C., Díez, P., Martín-Suárez, S., Rubio, M., Encinas, J.M., Fernández-Ruiz, J., Sagredo, O., 2021. Neuropathological characterization of a Dravet syndrome knock-in mouse model useful for investigating cannabinoid treatments. Front. Mol. Neurosci. 29, 602801.
Sharma, C., Al Kaabi, J.M., Nurulain, S.M., Goyal, S.N., Kamal, M.A., Ojha, S., 2016. Polypharmacological properties and therapeutic potential of β-caryophyllene: a dietary phytocannabinoid of pharmaceutical promise. Curr. Pharmaceut. Des. 22, 3237–3264.
Skluzacek, J.V., Watts, K.P., Parsy, O., Wical, B., Camfield, P., 2011. Dravet syndrome and parent associations: the IDEA League experience with comorbid conditions, mortality, management, adaptation, and grief. Epilepsia 52, 95–101.
Sullivan, J., Simmons, R., 2021. Fenfluramine for treatment-resistant epilepsy in Dravet syndrome and other genetically mediated epilepsies. Drugs Today 57, 449–454.
Tchekalarova, J., da Conceição Machado, K., Gomes Júnior, A.L., de Carvalho Melo Cavalcante, A.A., Momchilova, A., Tzoneva, R., 2018. Pharmacological characterization of the cannabinoid receptor 2 agonist, β-caryophyllene on seizure models in mice. Seizure 57, 22–26.
Thiele, E.A., Marsh, E.D., French, J.A., Mazurkiewicz-Beldzinska, M., Benbadis, S.R., Joshi, C., Lyons, P.D., Taylor, A., Roberts, C., Sommerville, K., GWPCARE4 Study Group, 2018. Cannabidiol in patients with seizures associated with Lennox-Gastaut syndrome (GWPCARE4): a randomised, double-blind, placebo-controlled phase 3 trial. Lancet 391, 1085–1096.
Thiele, E., Marsh, E., Mazurkiewicz-Beldzinska, M., Halford, J.J., Gunning, B., Devinsky, O., Checketts, D., Roberts, C., 2019. Cannabidiol in patients with Lennox-Gastaut syndrome: interim analysis of an open-label extension study. Epilepsia 60, 419–428.
Valdeolivas, S., Sagredo, O., Delgado, M., Pozo, M.A., Fernández-Ruiz, J., 2017. Effects of a Sativex-like combination of phytocannabinoids on disease progression in R6/2 mice, an experimental model of Huntington's disease. Int. J. Mol. Sci. 18, 684.
Vezzani, A., French, J., Bartfai, T., Baram, T.Z., 2011. The role of inflammation in epilepsy. Nat. Rev. Neurol. 7, 31–40.
Vezzani, A., Balosso, S., Ravizza, T., 2019. Neuroinflammatory pathways as treatment targets and biomarkers in epilepsy. Nat. Rev. Neurol. 15, 459–472.
Villas, N., Meskis, M.A., Goodliffe, S., 2017. Dravet syndrome: characteristics, comorbidities, and caregiver concerns. Epilepsy Behav. 74, 81–86.
Viveros-Paredes, J.M., González-Castañeda, R.E., Gertsch, J., Chaparro-Huerta, V., López-Roa, R.I., Vázquez-Valls, E., Beas-Zarate, C., Camins-Espuny, A., Flores-Soto, M.E., 2017. Neuroprotective effects of β-caryophyllene against dopaminergic neuron injury in a murine model of Parkinson's disease induced by MPTP. Pharmaceuticals 10, 60.
Wirrell, E.C., Laux, L., Donner, E., Jette, N., Knupp, K., Meskis, M.A., Miller, I., Sullivan, J., Pharm, M.W., Berg, A.T., 2017. Optimizing the diagnosis and management of Dravet syndrome: recommendations from a North American consensus panel. Pediatr. Neurol. 68, 18–34.
Wu, C., Jia, Y., Lee, J.H., Jun, H.J., Lee, H.S., Hwang, K.Y., Lee, S.J., 2014. trans-Caryophyllene is a natural agonistic ligand for peroxisome proliferator-activated receptor-α. Bioorg. Med. Chem. Lett 24, 3168–3174.
Wu, Y.W., Sullivan, J., McDaniel, S.S., Meisler, M.H., Walsh, E.M., Li, S.X., Kuzniewicz, M.W., 2015. Incidence of Dravet syndrome in a US population. Pediatrics 136, e1310–e1315.
Youssef, D.A., El-Fayoumi, H.M., Mahmoud, M.F., 2019. Beta-caryophyllene alleviates diet-induced neurobehavioral changes in rats: the role of CB2 and PPAR-γ receptors. Biomed. Pharmacother. 110, 145–154.